Dynamic Axial Chirality of Ferrocene Diamino Acids: Hydration Effects and Chiroptical Applications

Zhaohui Zong,† Zhaozhen Cao, † Aiyou Hao* and Pengyao Xing*

School of Chemistry and Chemical Engineering, Shandong University, Jinan 250100, PR China. Email: haoay@sdu.edu.cn; xingpengyao@sdu.edu.cn

†These authors contributed equally to this work.

Experimental section

Materials

(1R)-(-)-Myrtenal and (S)-(-)-Perillaldehyde were purchased from Shanghai Macklin Biochemical Technology Co., Ltd. (-)-Citronellal was purchased from Shanghai Jiuding Chemical Technology Co., Ltd. (R)-(+)-Citronellal was purchased from Aldrich Chemical Co., Inc. Other chemicals were purchased from HEOWNS Biochemical Technology Co., LTD, China. All reagents were used without further purification in this work. All water used in this work was deionized (DI) water.

Characterizations

^{1}HNMR spectra, ^{13}C NMR spectra and 2D ROSEY were obtained by BRUKER AVANCE III HD 400. Temperature-variable ^{1}HNMR spectra and ROESY spectra were carried out by BRUKER AVANCE III 500. High-Resolution Mass Spectra (HR-MS) were performed on an Agilent Q-TOF 6510. CD, temperature-variable CD and CPL were measured with an Applied Photophysics ChirascanV100 model. Single crystal data were collected on a Rigaku XtaLAB Synergy.

Computational details

For all of different angles of Ala (0-360 ^{o} and 72-108^{o}) were constructed by Gaussian view 06. Other compound structures were obtained from the single crystal structures. All of ground-state geometry of Ala was optimized using hf/6-31g basic set. Notably, in order to make sure certain angle between two CP rings, the atoms of ferrocene and the carbon atoms of the carbonyl group directly connected to the CP ring were fixed while other atoms were allowed to optimize without freeze. Base on the optimized geometry, time-dependent density functional theory (TDDFT) with Becke's three-parameter exchange Lee-Yang-Parr correlation functional (B3LYP) and 6-311g(d) basis set were employed to calculate ECD using the Gaussian 16 program.

All of Ala conformations with different angles (0-360^{o} and 72-108^{o}) were constructed by Gaussian view 06. Other structures were obtained from the single crystal structures. All of the ground-state geometries of Ala were optimized using b3lyp/6-311g(d) basic set. Notably, in order to determine certain angles between two CP rings, the atoms of ferrocene and the carbon atoms of the carbonyl group directly connected to the CP ring were fixed while other atoms were allowed to optimize without freeze, and water was used a PCM solvation model. The convergence criteria of optimization are as follows: Maximum Force 0.000015, RMS Force 0.000010, Maximum Displacement 0.000060, RMS Displacement 0.000040. To ensure that the optimized geometry was at a minimum, all geometry optimizations were followed by a frequency calculation and only positive frequencies were obtained and hessian matrix can be obtained. The thermodynamic data including electronic Energy (EE) + Thermal Free Energy Correction was calculated at b3lyp/6-311g(d) level of theory.

The optimization of Ala in water was carried out at b3lyp/6-311g(d) level. Especially, A few water molecules positions were modified artificially for better simulation after initial structure with 11 water molecules was given by Gromacs 2020 program. Then the calculations were performed with water PCM solvation model.

Synthesis of ferrocene diamino acids

The synthesis route was based on the following Scheme S1. 1,1'-Ferrocenedicarboxylic Acid (600 mg) and L-alanine methyl ester hydrochloride (1500 mg) with HOBT (300 mg), DMAP (300 mg), EDC (1200 mg), TEA (1 mL) were stirred in DMF (60 mL) at room temperature for 8 h. After the reaction completed, poured the DMF solution into acidic water. Then crude product was extracted by DCM by three times, and dried by anhydrous $MgSO_4$. Next, crude product was purified by silica gel column (DCM : MeOH 100:1). The final product was obtained by hydrolysis reaction with LiOH (1.5g) in THF aqueous solution (1:1). Other compounds were obtained by the same methods. ^{1}H NMR, ^{13}C NMR and high-resolution Mass spectra (HRMS) can be found in Fig. S1-S35.

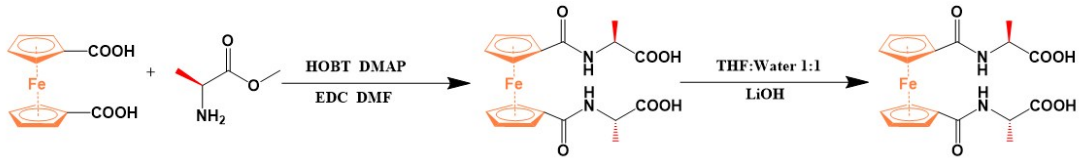

Scheme S1. Synthesis route of ferrocene diamino acid derivatives.

Synthesis of ferrocene-glycine hydrazine derivative (Scheme S2)

200 mg Gly methyl ester was dissolved in 20 ml dry methanol. Hydrazine hydrate (3 mL) was added and the mixture was stirred overnight. The product was obtained after

the solvents were evaporated in *vacuo*.

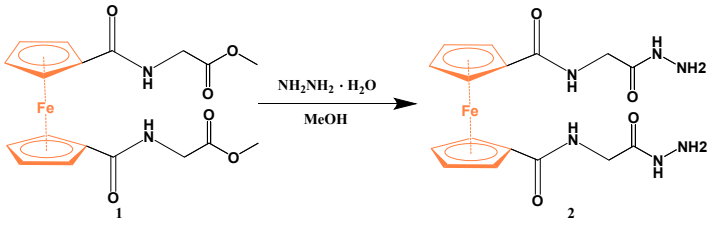

Scheme S2. Synthesis route of ferrocene-glycine hydrazine derivative.

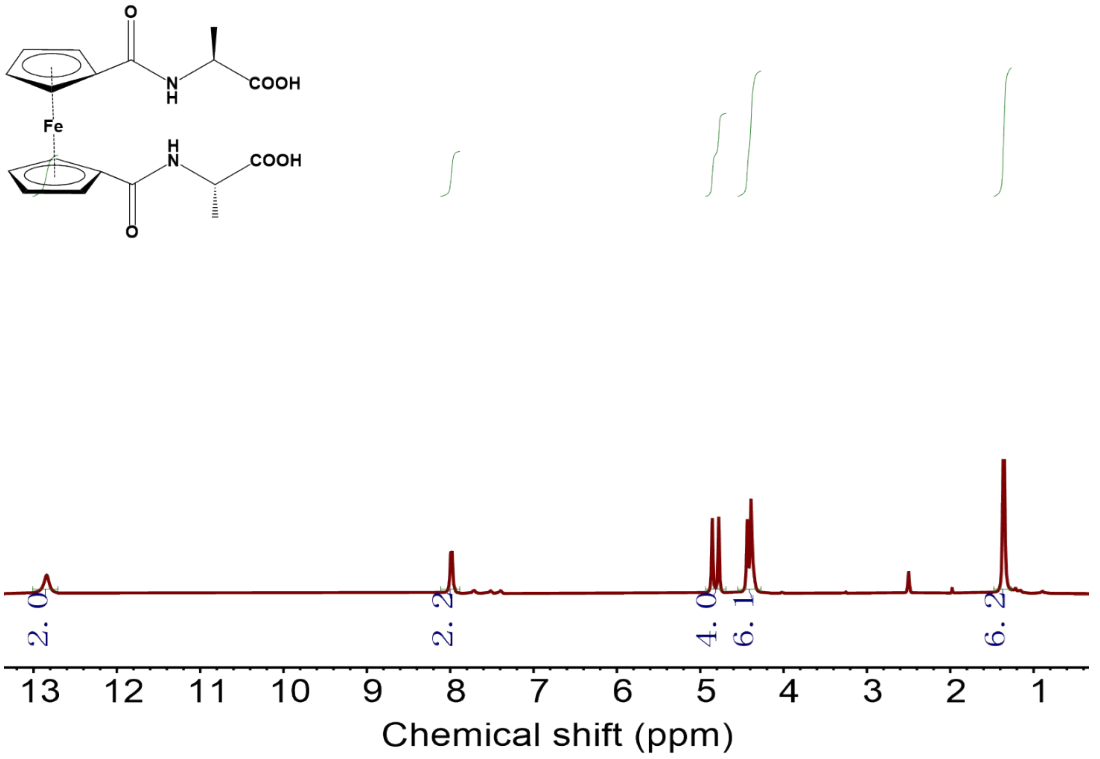

Figure S1. ^{1}H NMR spectrum of Ala.

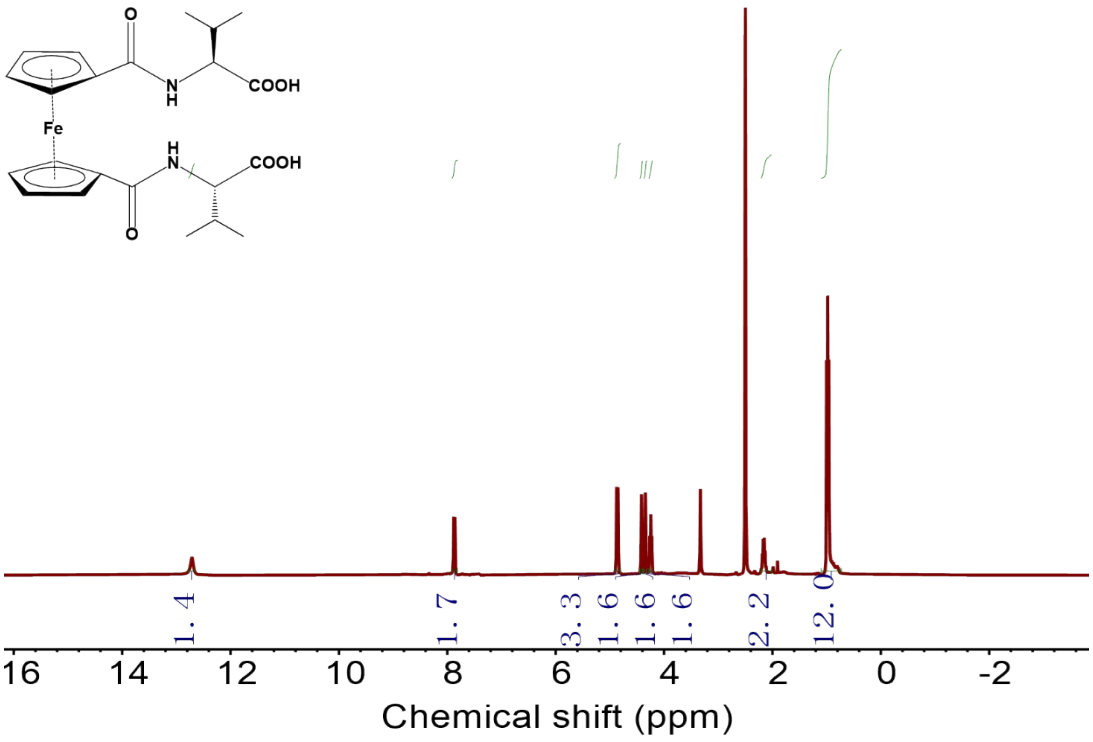

Figure S2. ^{1}H NMR spectrum of Val.

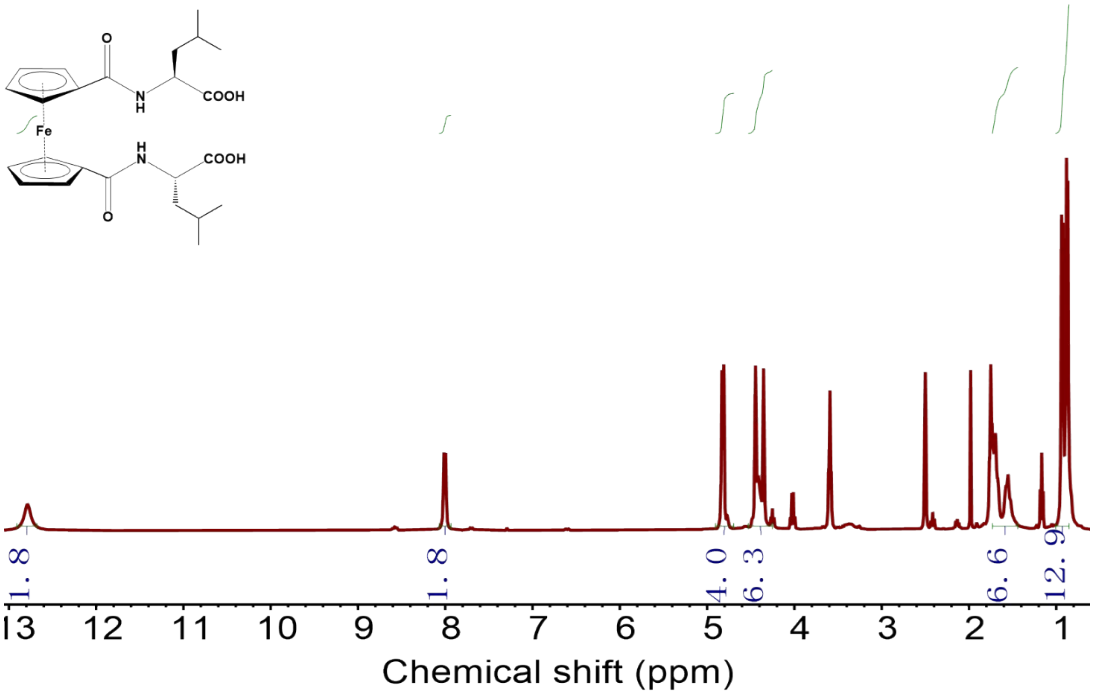

Figure S3. ^{1}H NMR spectrum of Leu.

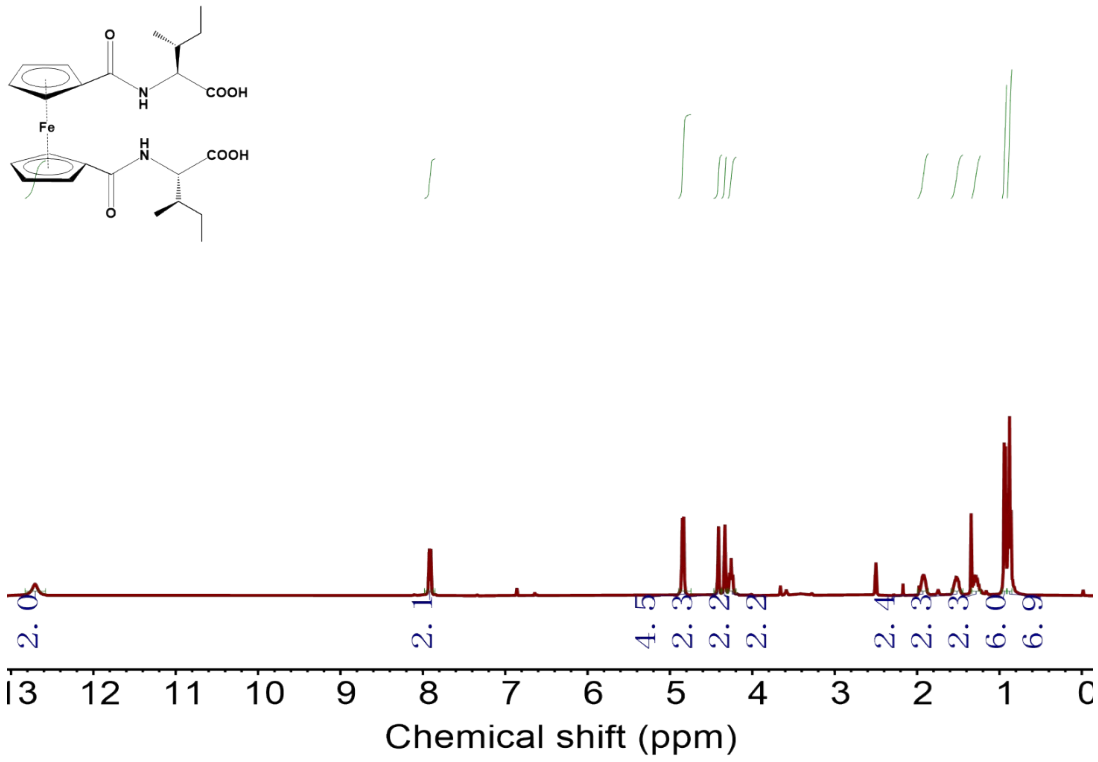

Figure S4. ^{1}H NMR spectrum of Ile.

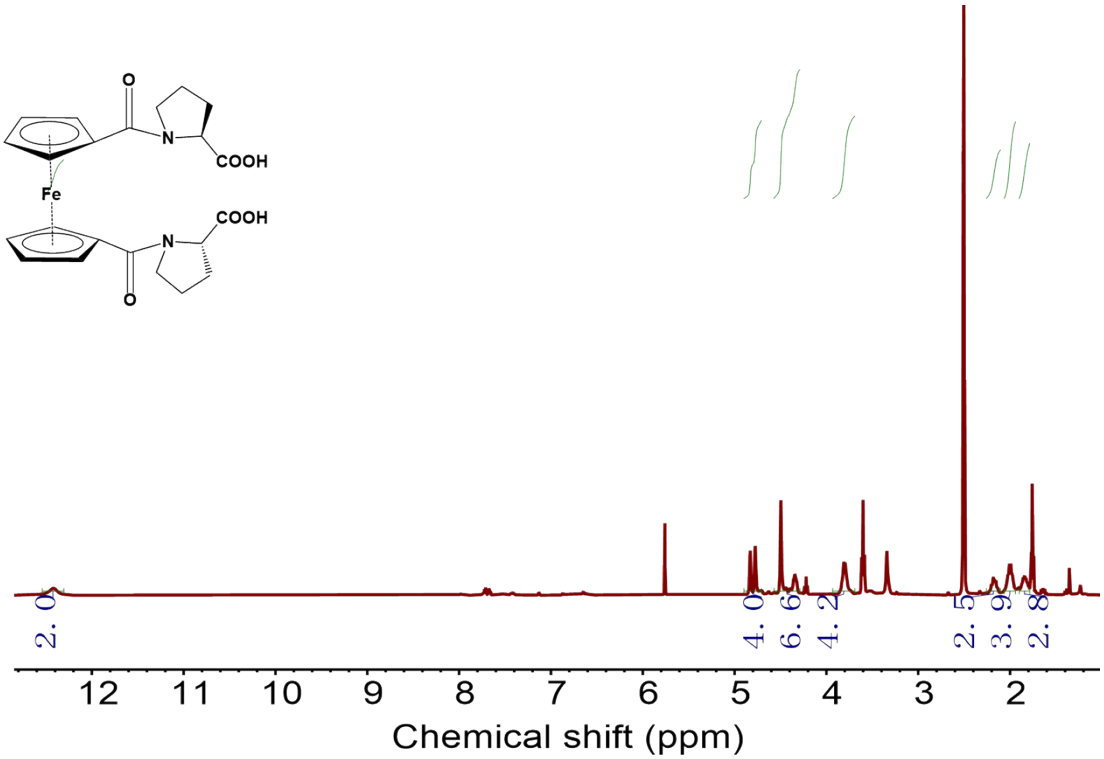

Figure S5. ^{1}H NMR spectrum of Pro.

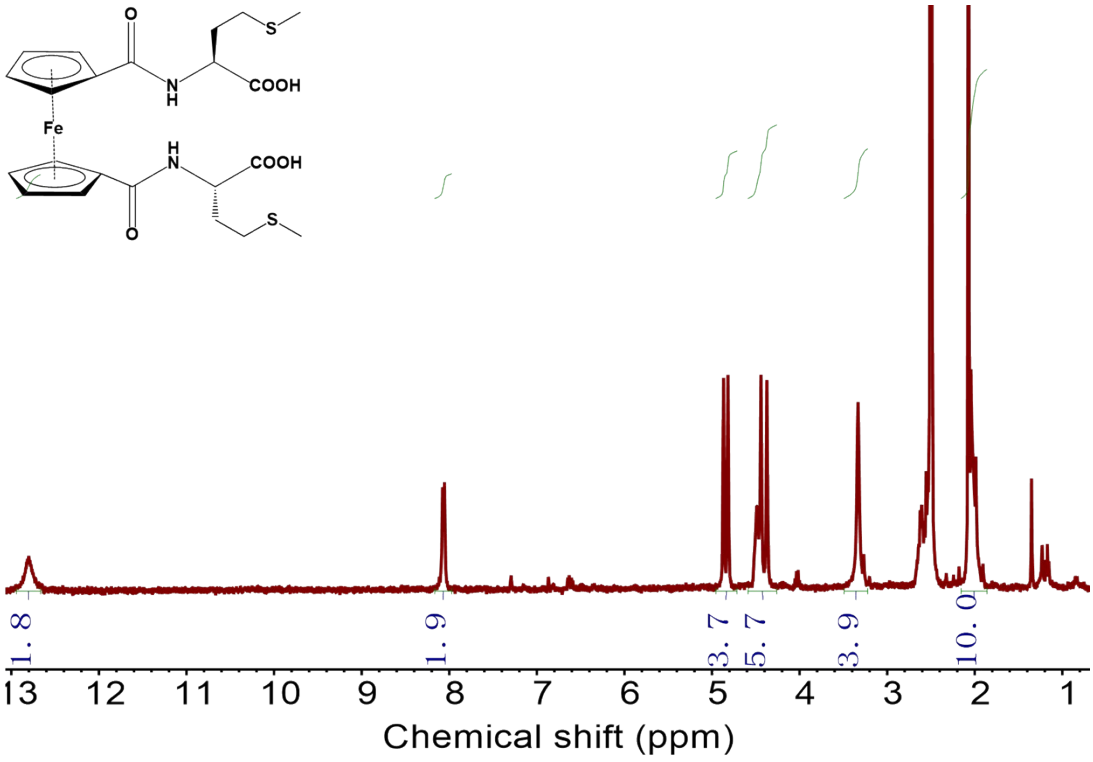

Figure S6. ^{1}H NMR spectrum of Met.

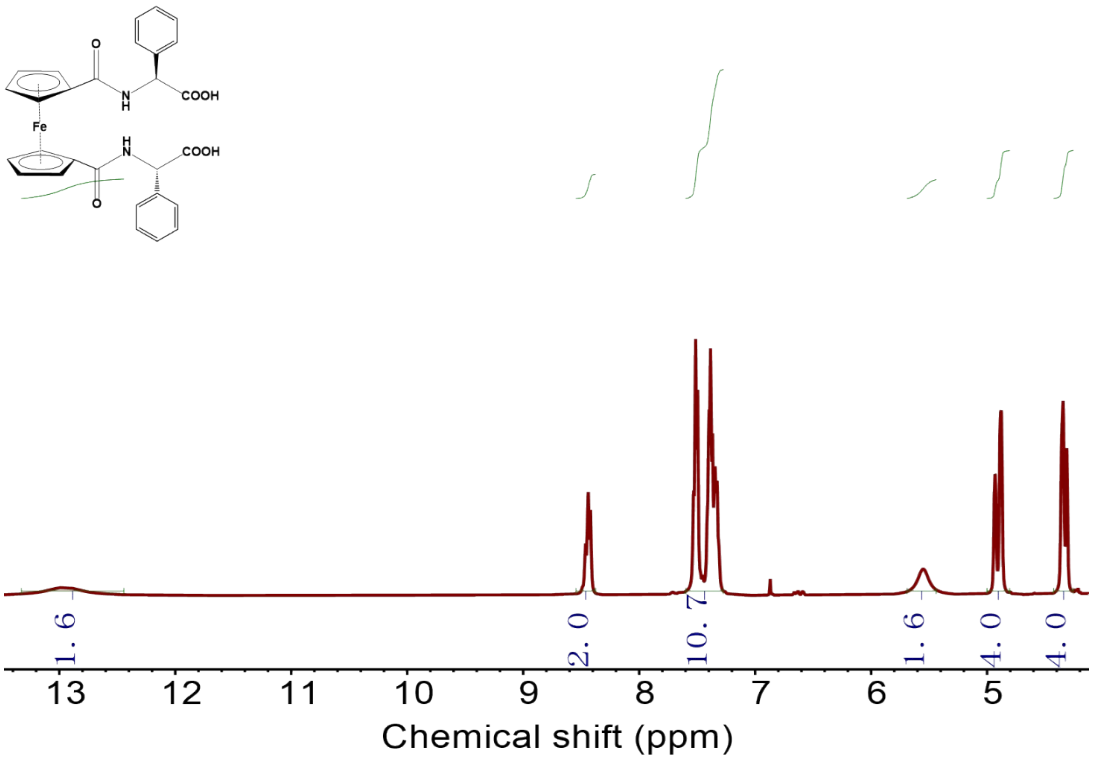

Figure S7. ^{1}H NMR spectrum of PGly.

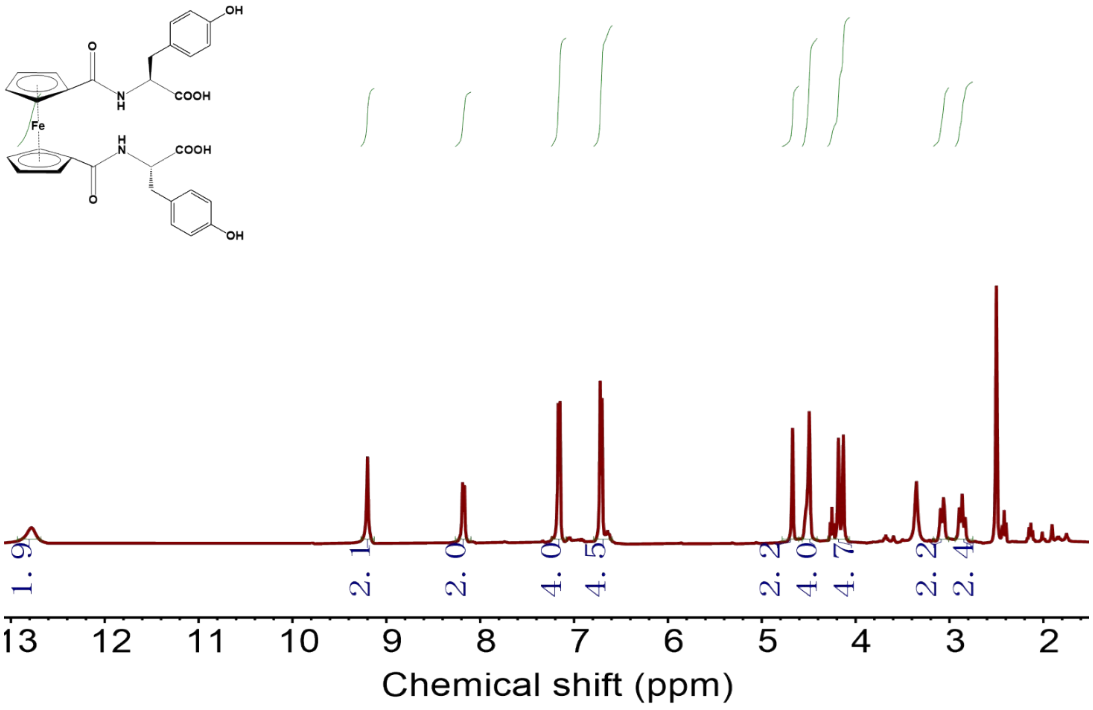

Figure S8. ^{1}H NMR spectrum of Tyr.

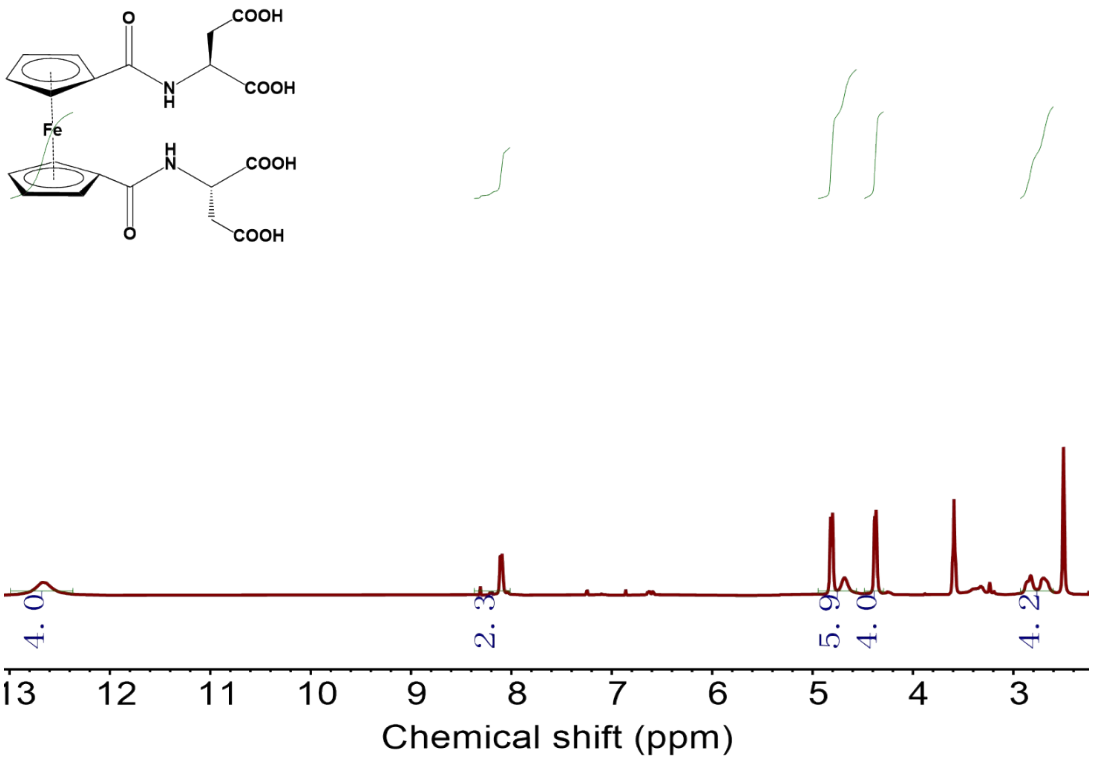

Figure S9. ^{1}H NMR spectrum of Asp.

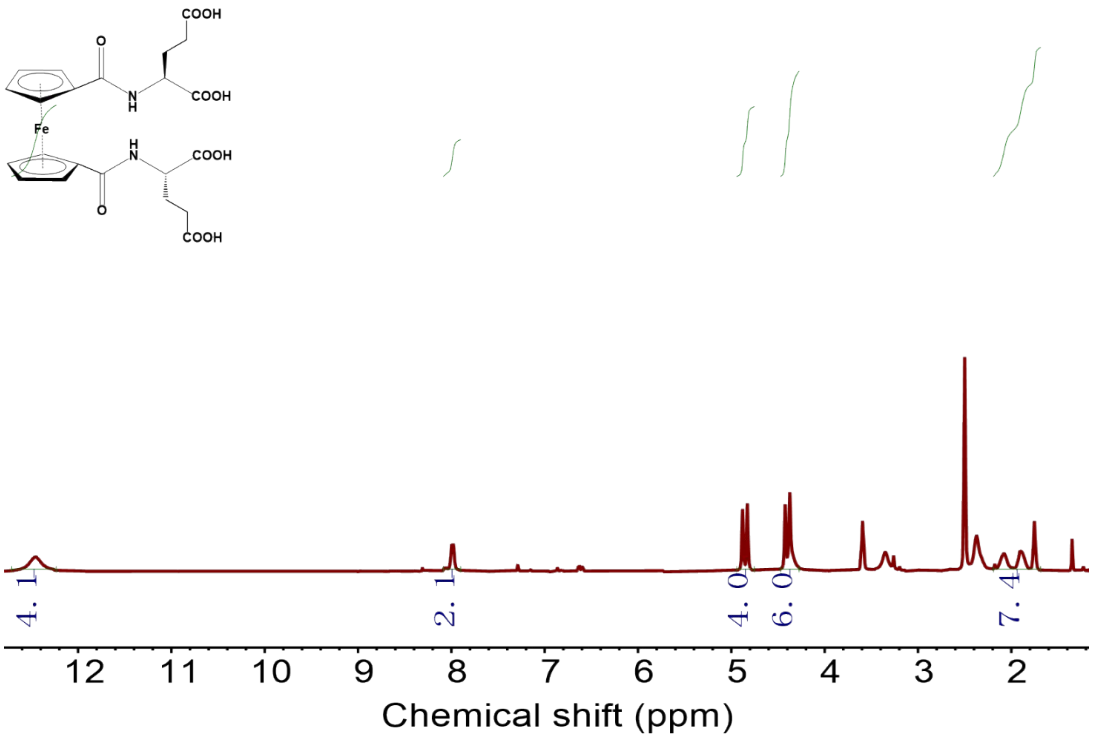

Figure S10. ^{1}H NMR spectrum of Glu.

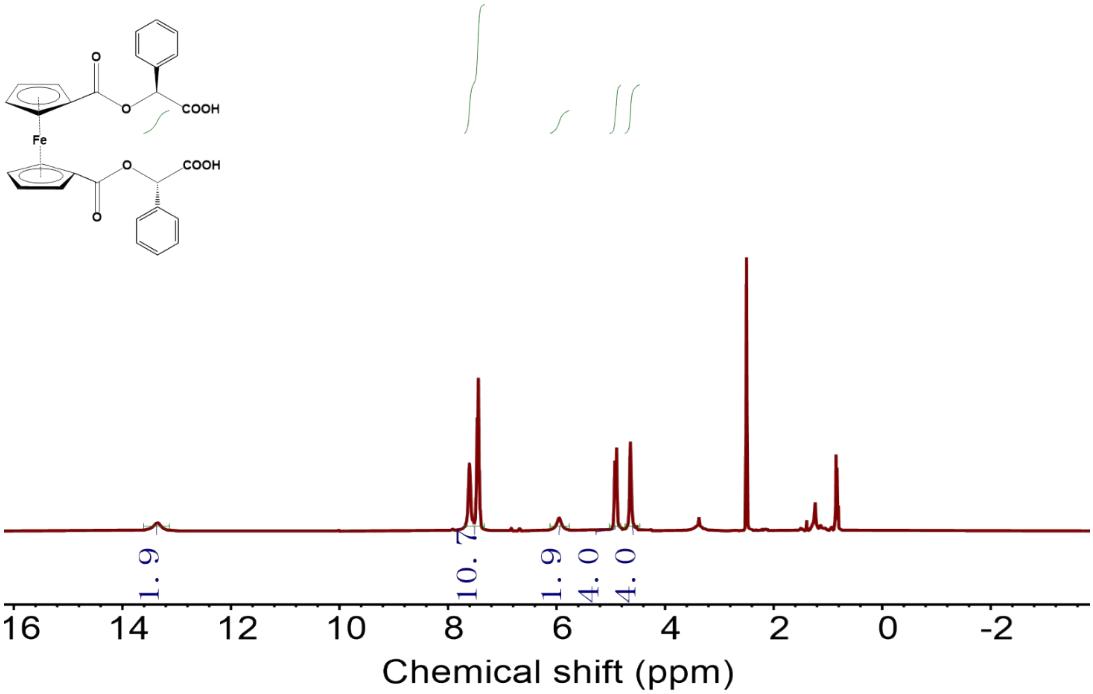

Figure S11. ^{1}H NMR spectrum of Man.

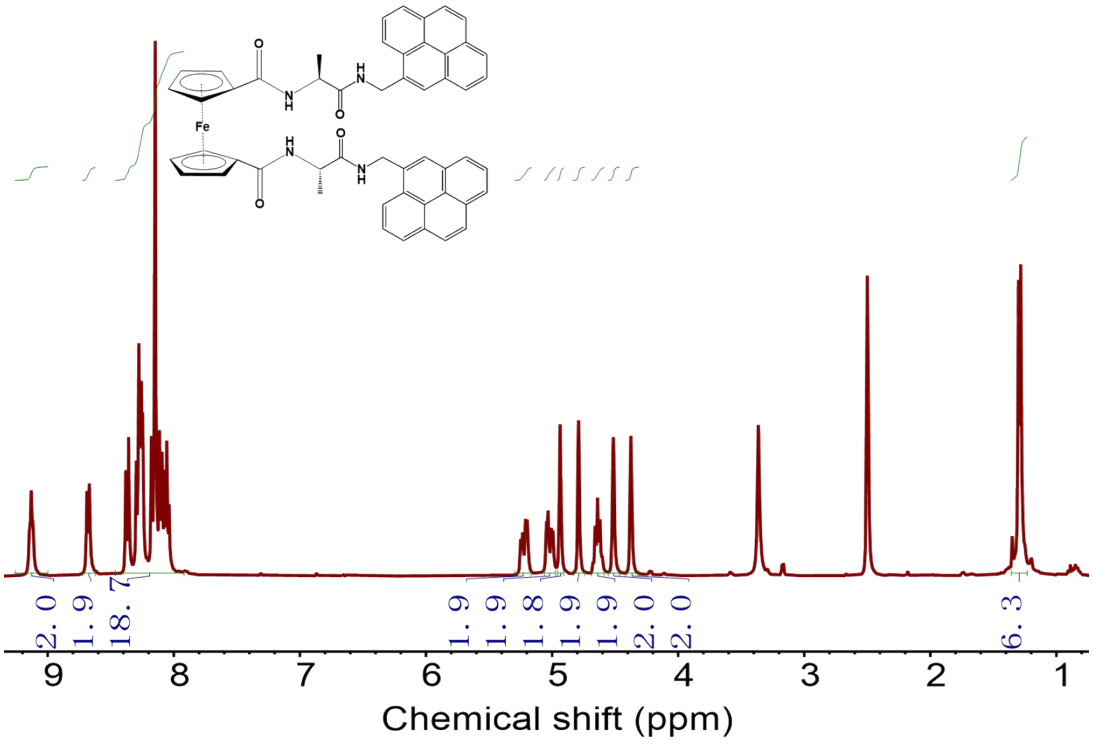

Figure S12. ^{1}H NMR spectrum of Ala-Py.

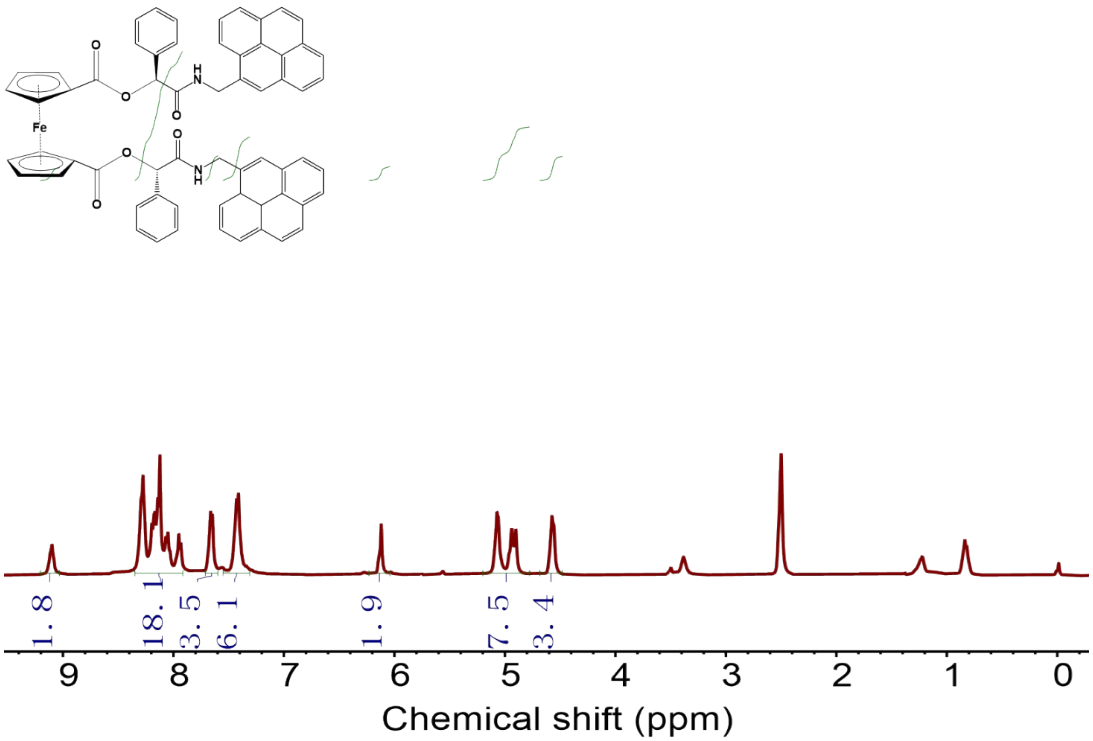

Figure S13. ^{1}H NMR spectrum of Man-Py.

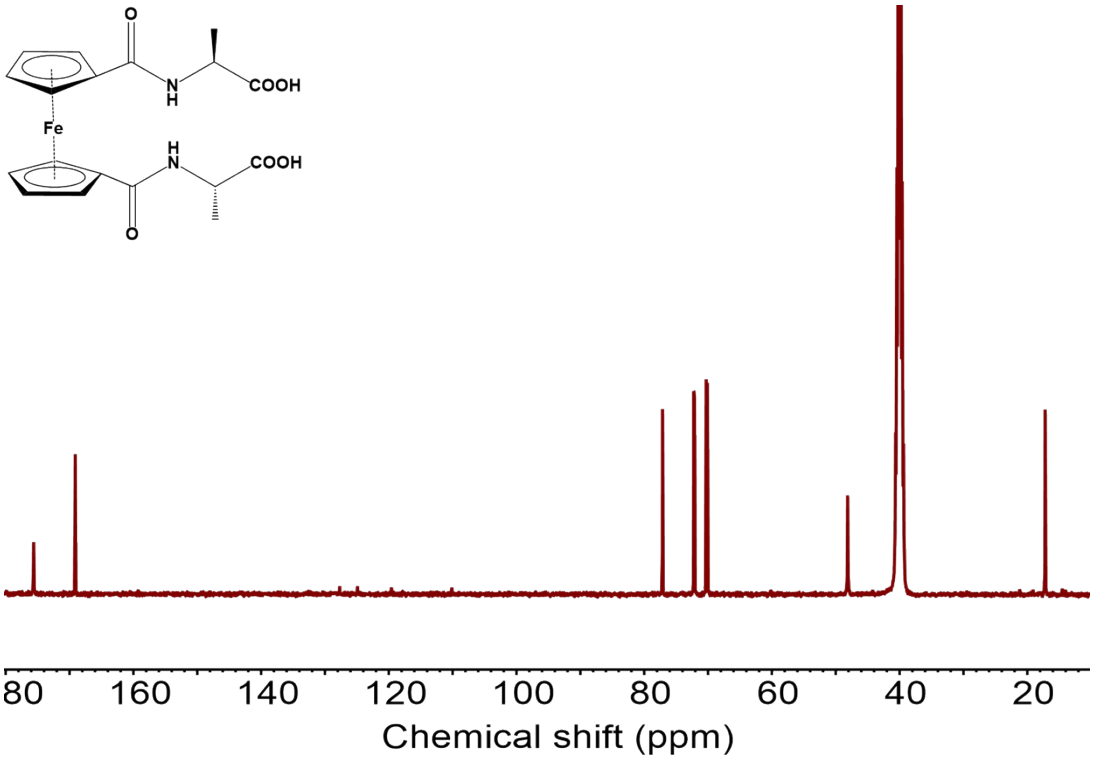

Figure S14. ^{13}C NMR spectrum of Ala.

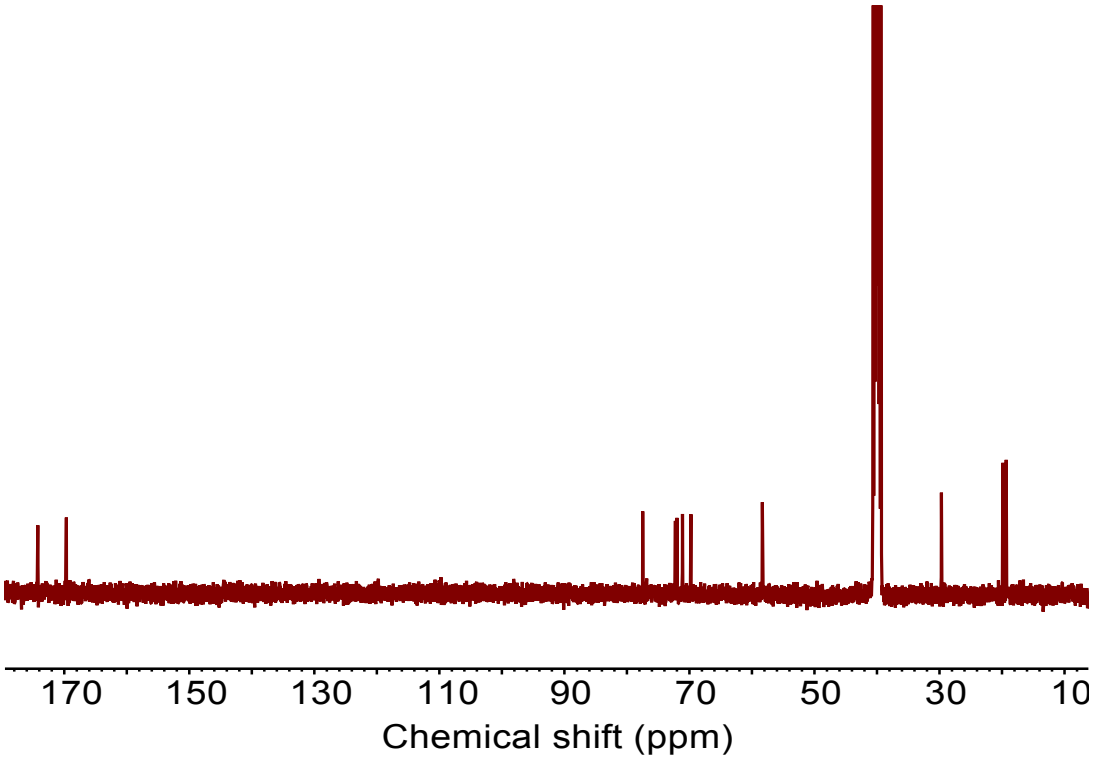

Figure S15. ^{13}C NMR spectrum of Val.

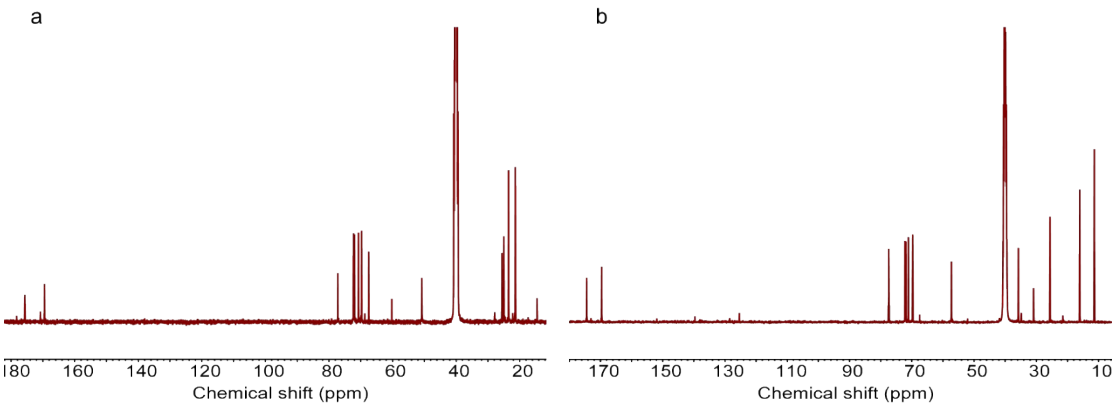

Figure S16. **a** ^{13}C NMR spectrum of Leu. **b** ^{13}C NMR spectrum of Ile.

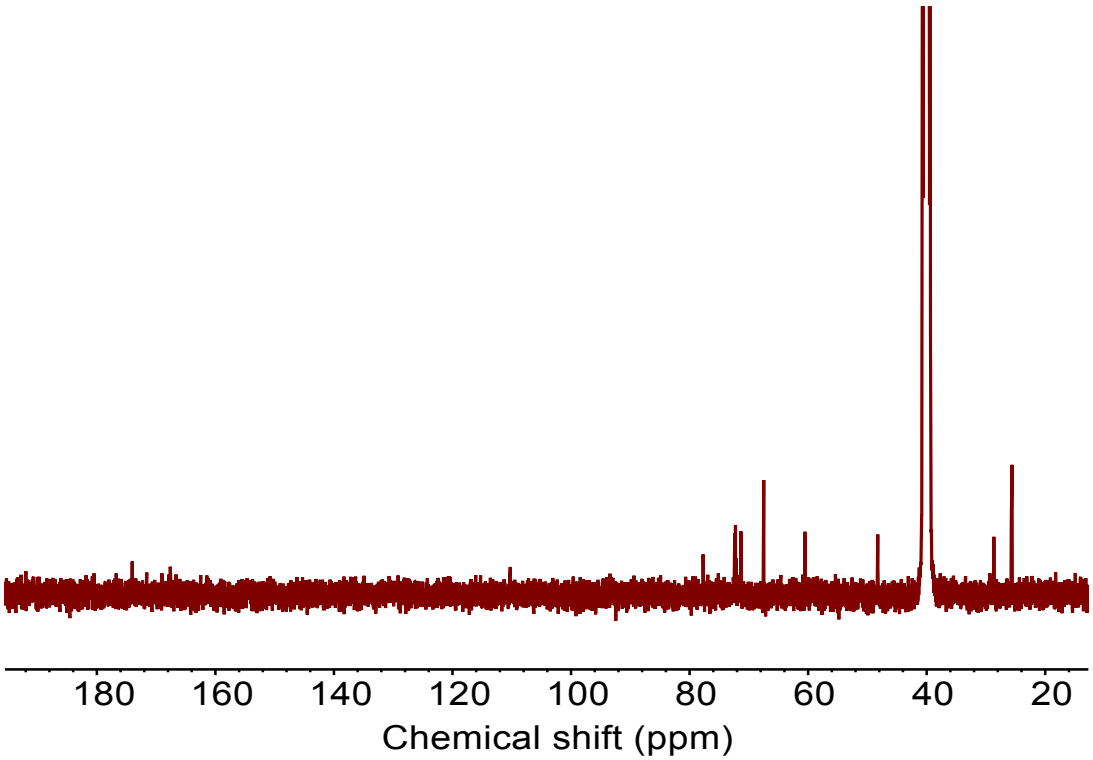

Figure S17. ^{13}C NMR spectrum of Pro.

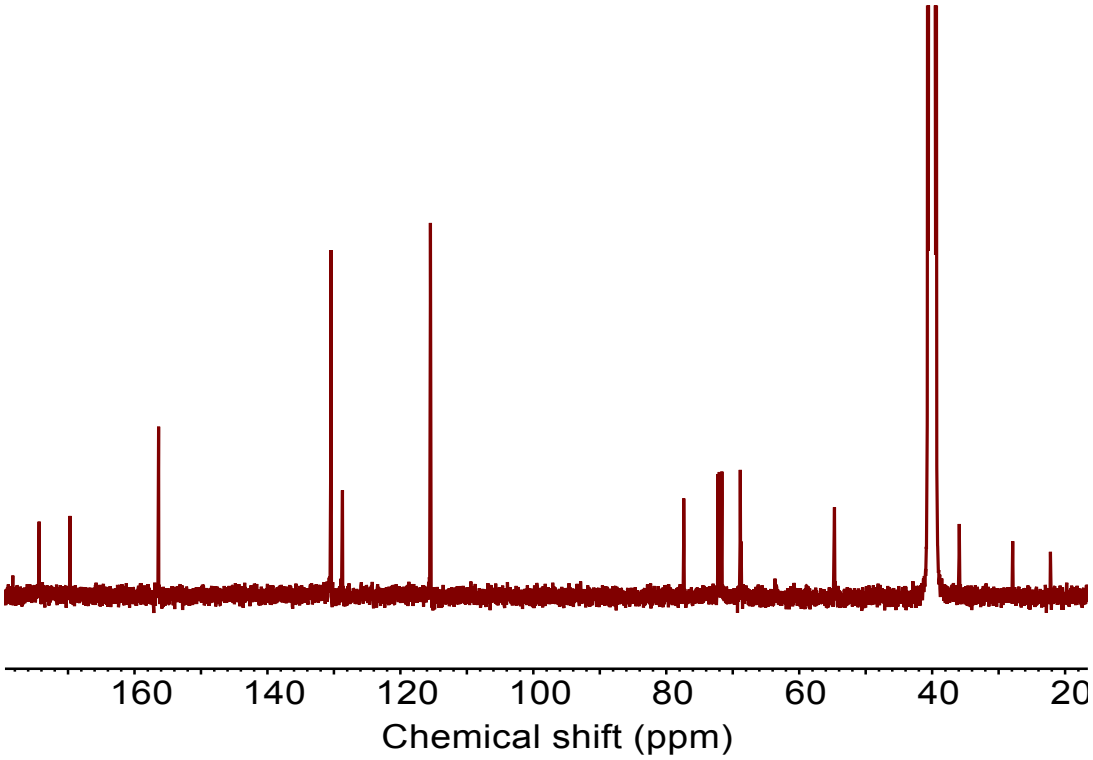

Figure S18. ^{13}C NMR spectrum of Tyr.

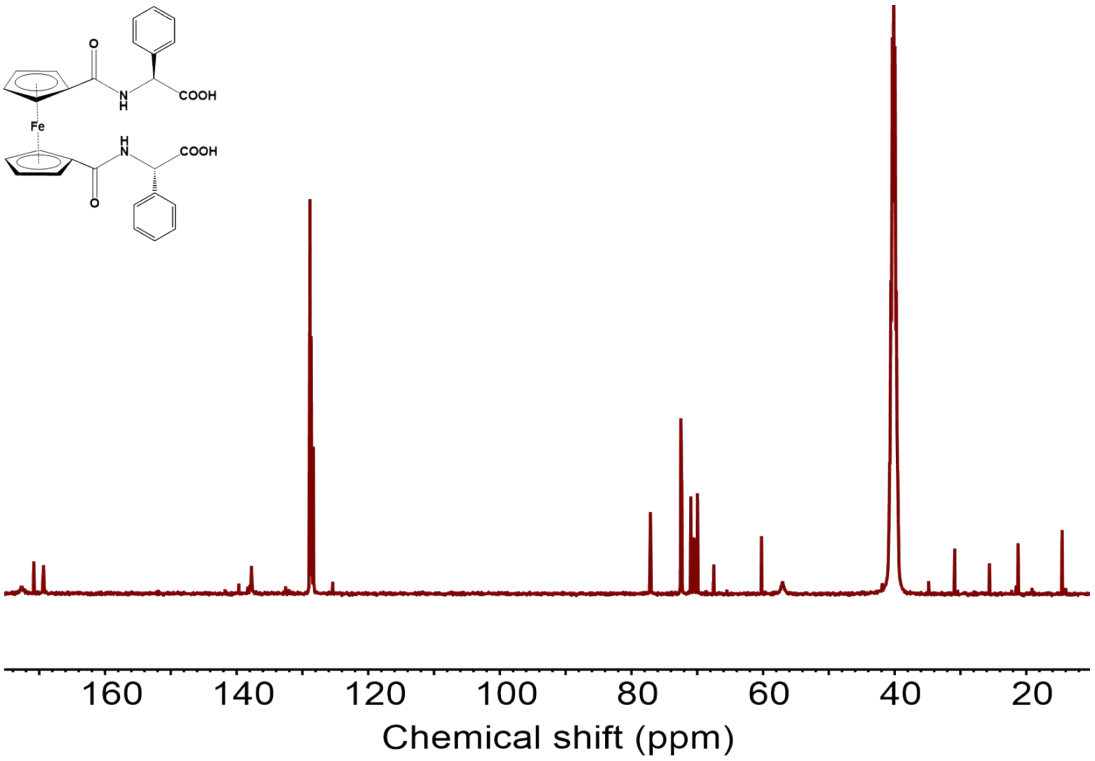

Figure S19. ^{13}C NMR spectrum of PGly.

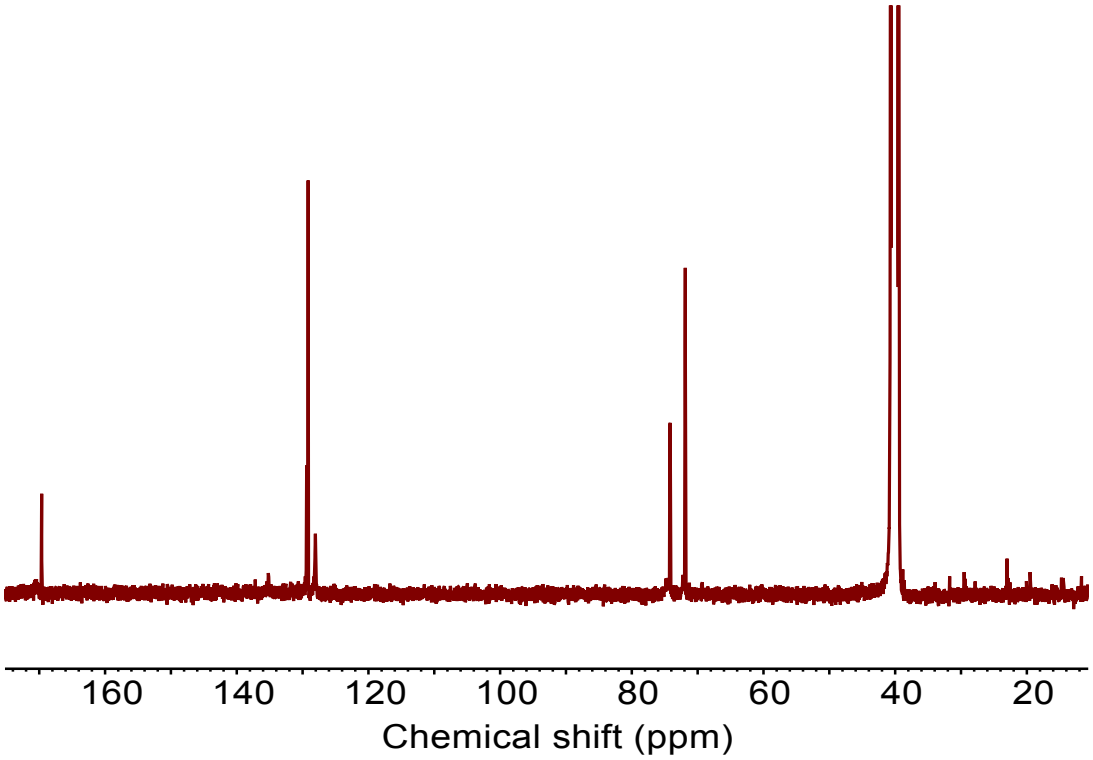

Figure S20. ^{13}C NMR spectrum of Man.

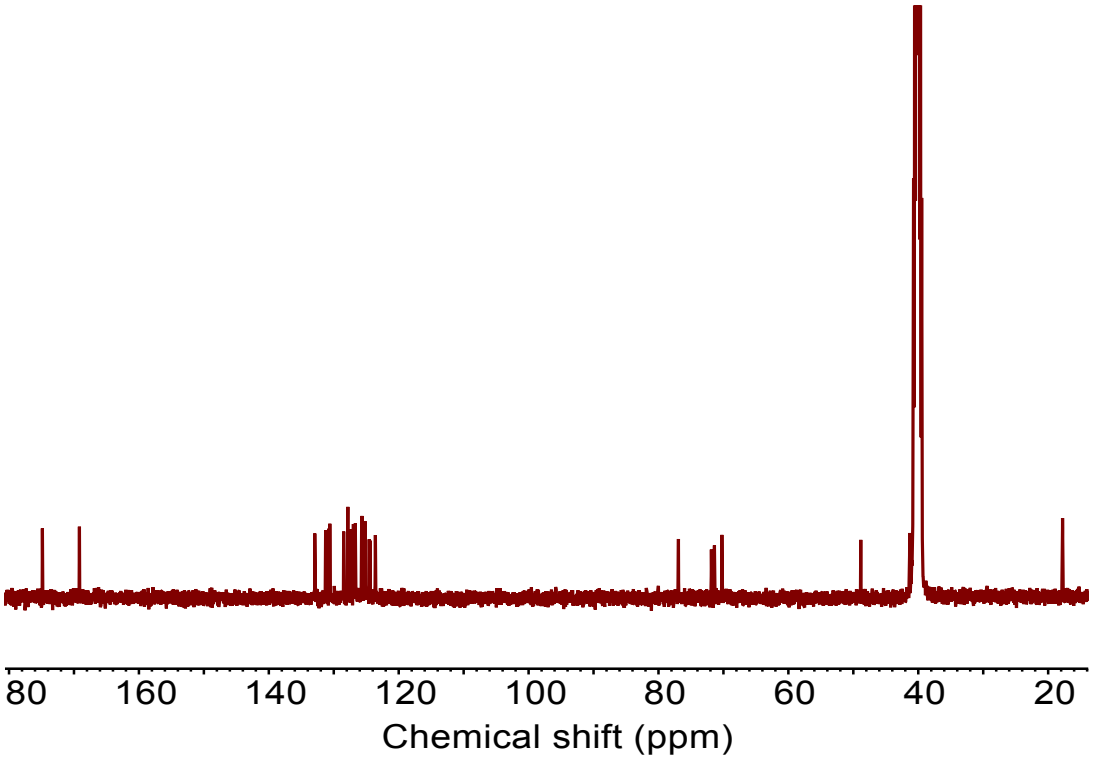

Figure S21. ^{13}C NMR spectrum of Ala-Py.

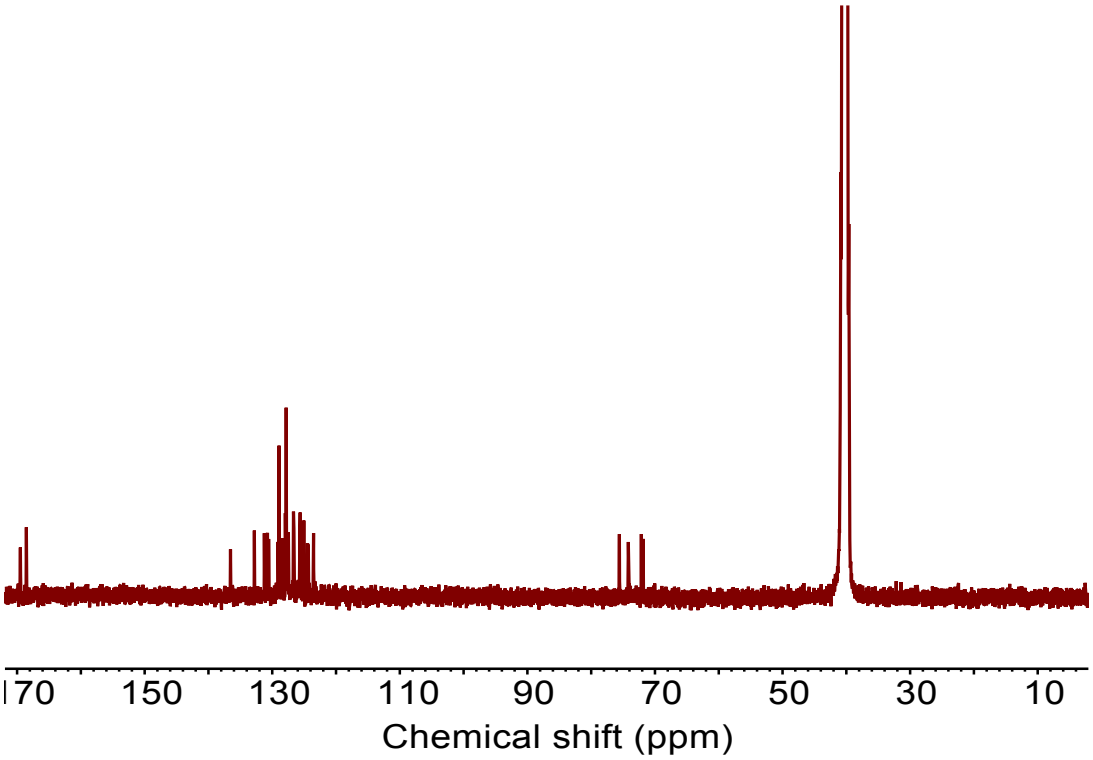

Figure S22. ^{13}C NMR spectrum of Man-Py.

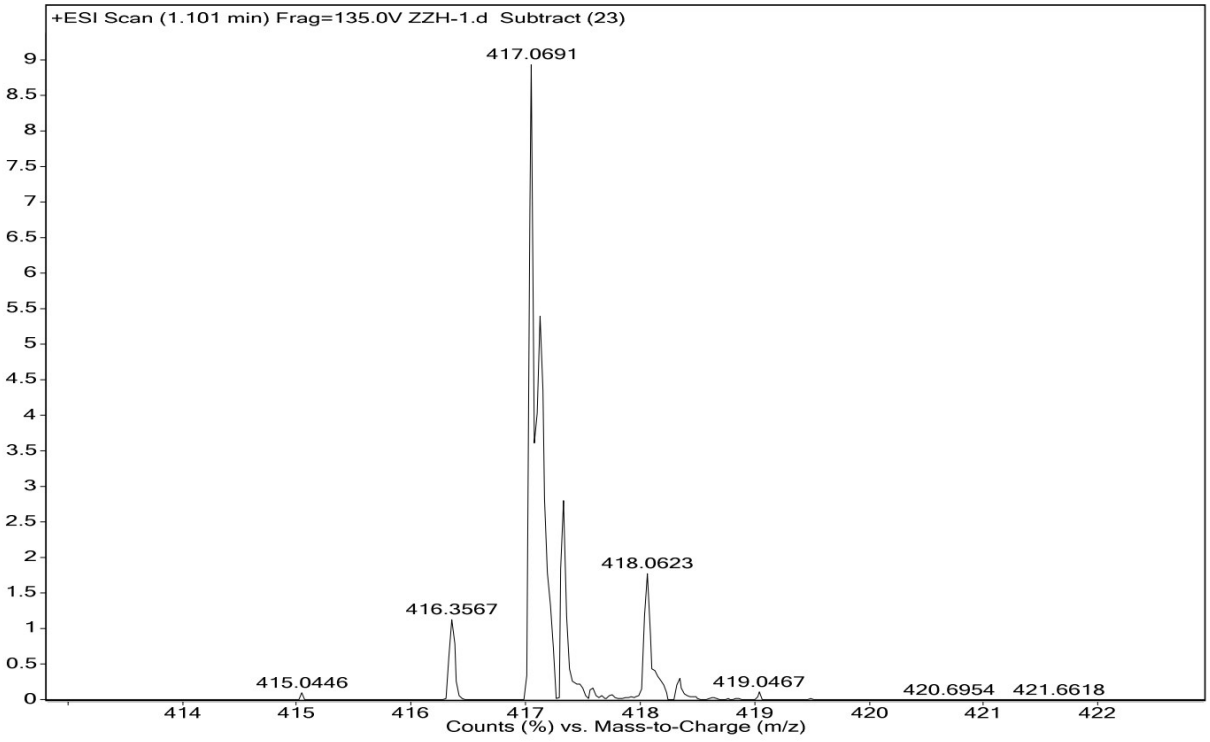

Figure S23. HRMS spectrum of Ala.

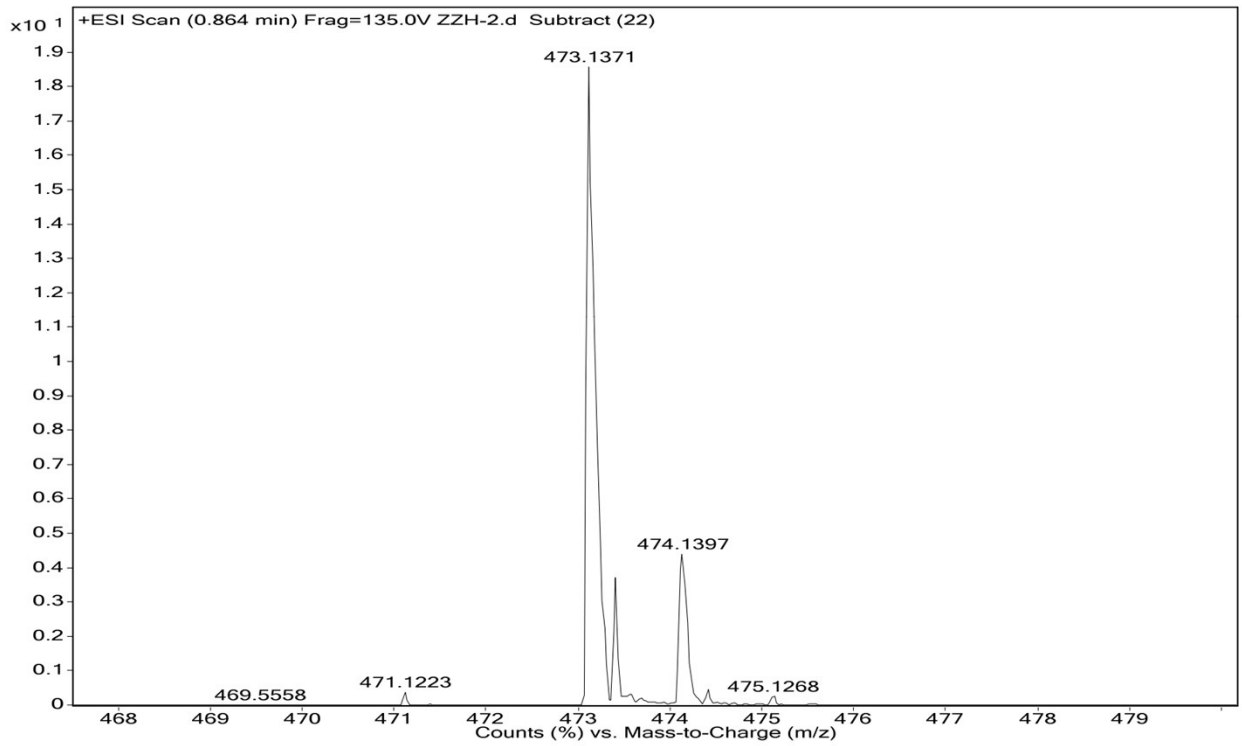

Figure S24. HRMS spectrum of Val.

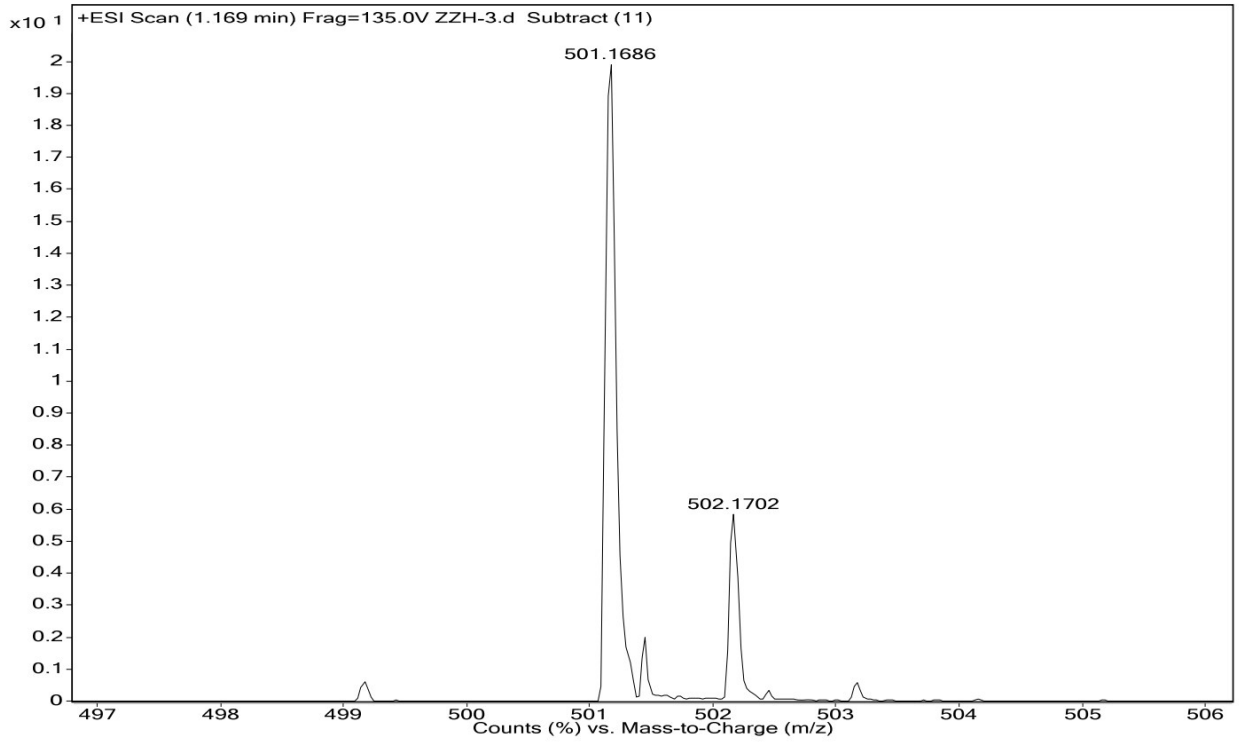

Figure S25. HRMS spectrum of Leu.

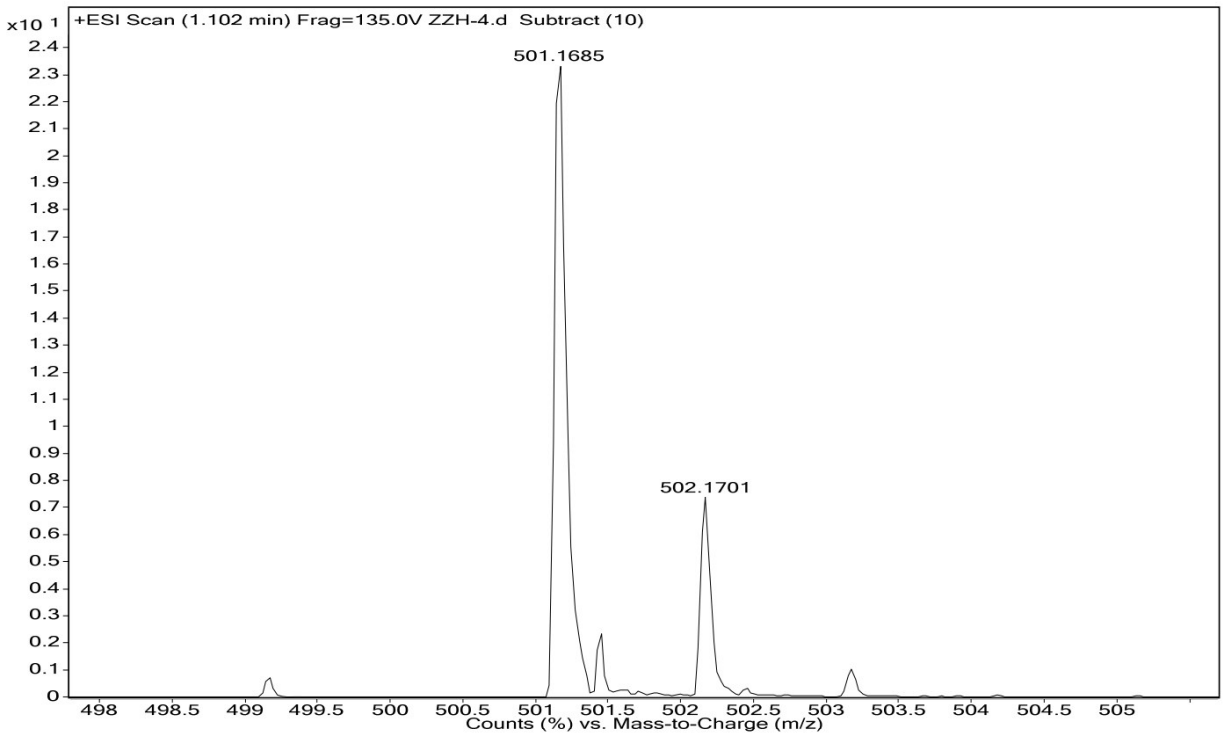

Figure S26. HRMS spectrum of Ile.

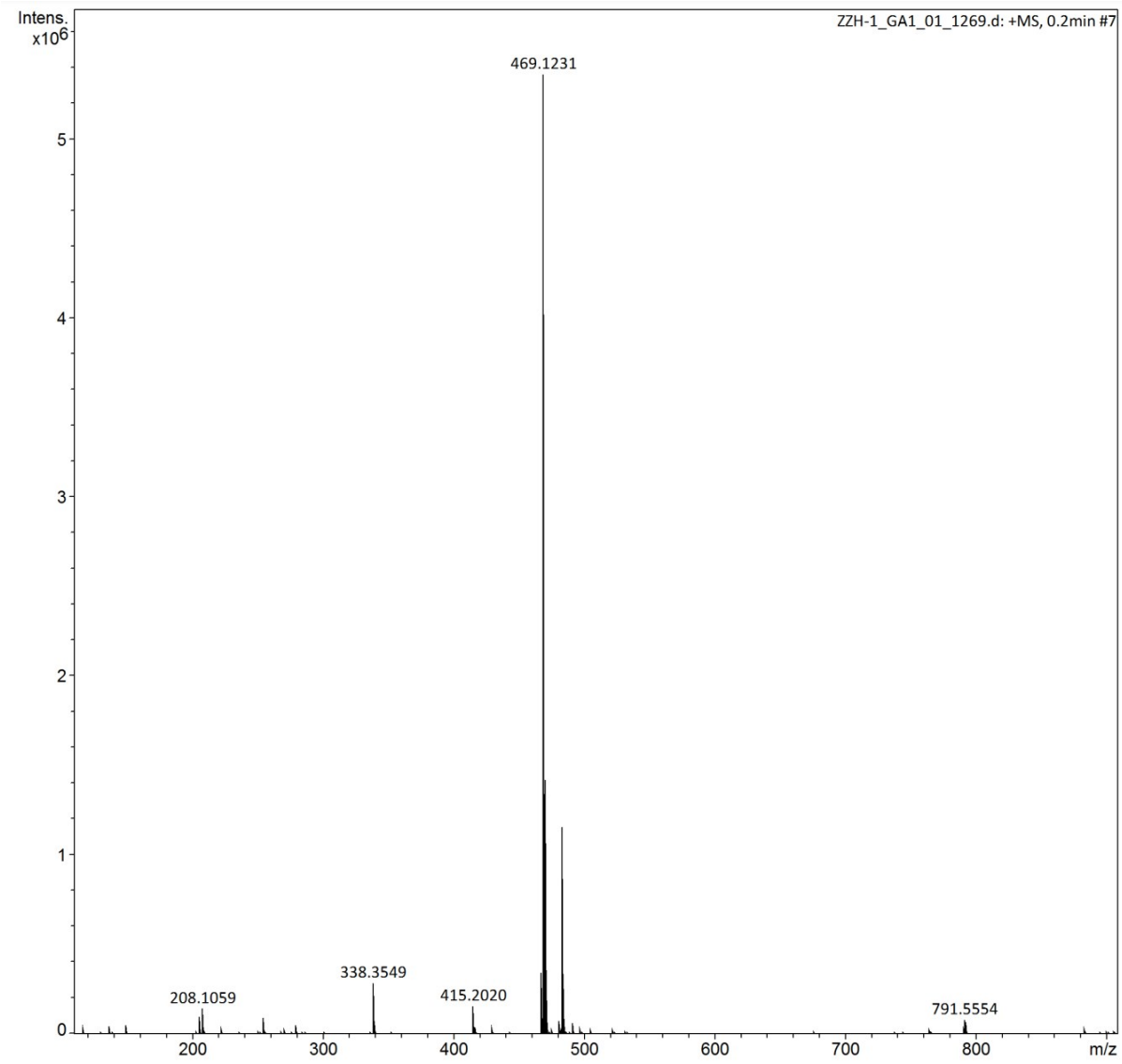

Figure S27. HRMS spectrum of Pro.

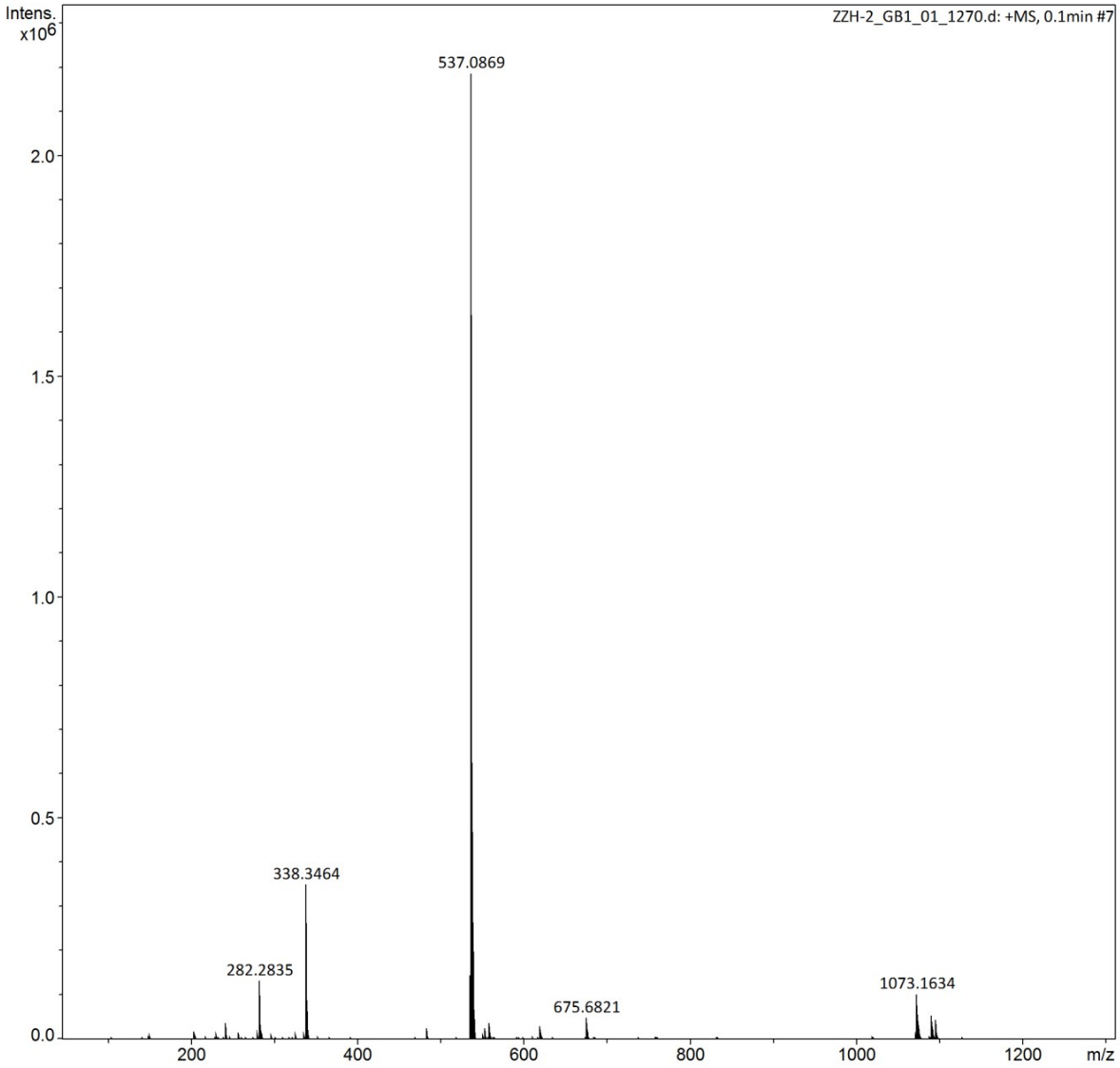

Figure S28. HRMS spectrum of Met.

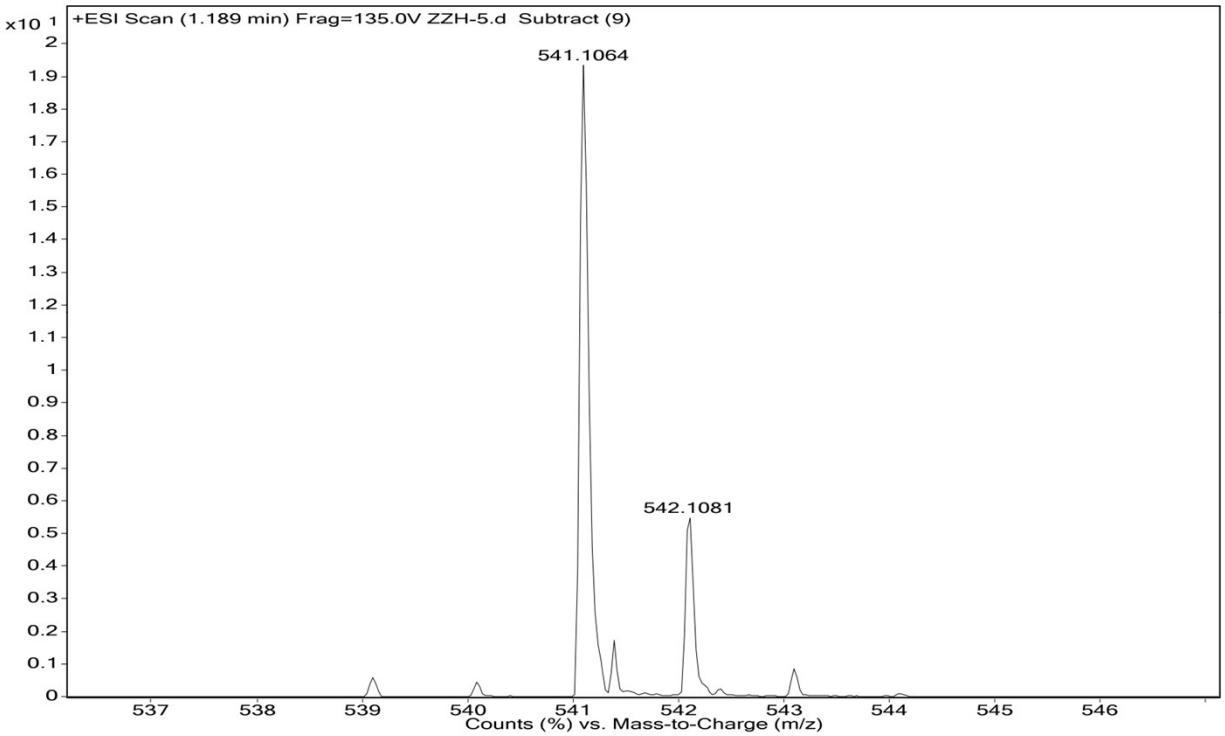

Figure S29. HRMS spectrum of PGly.

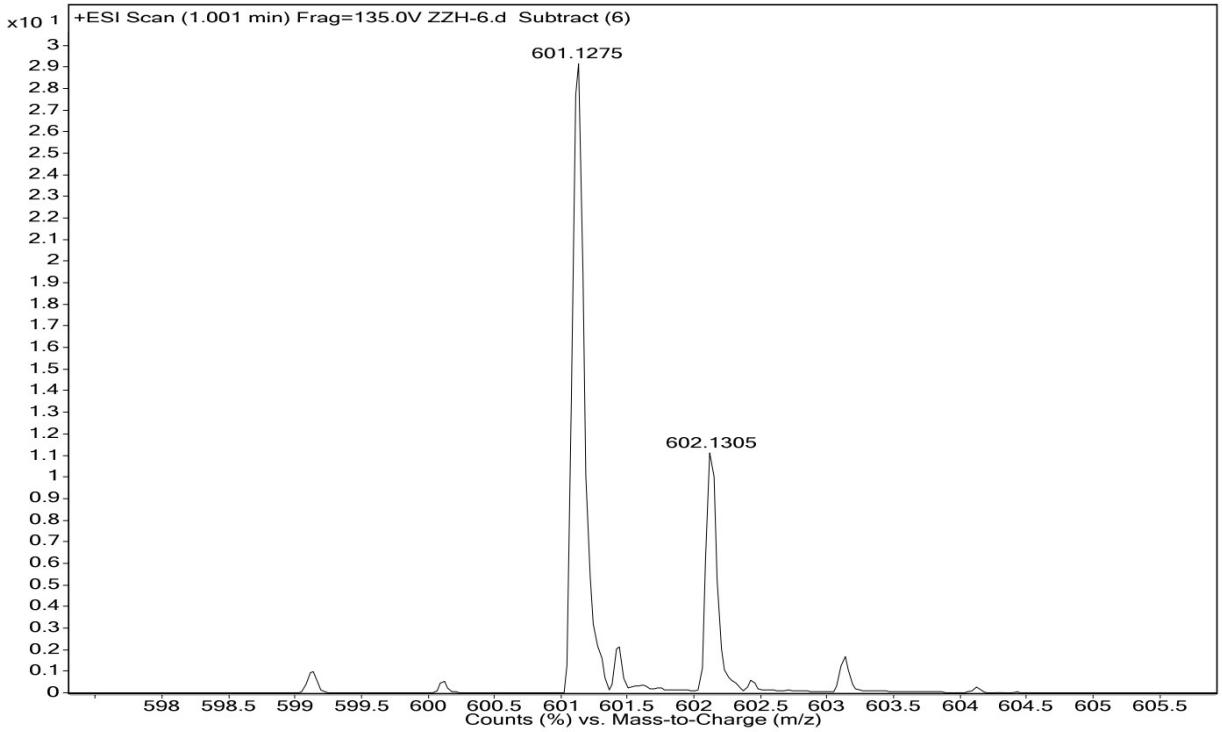

Figure S30. HRMS spectrum of Tyr.

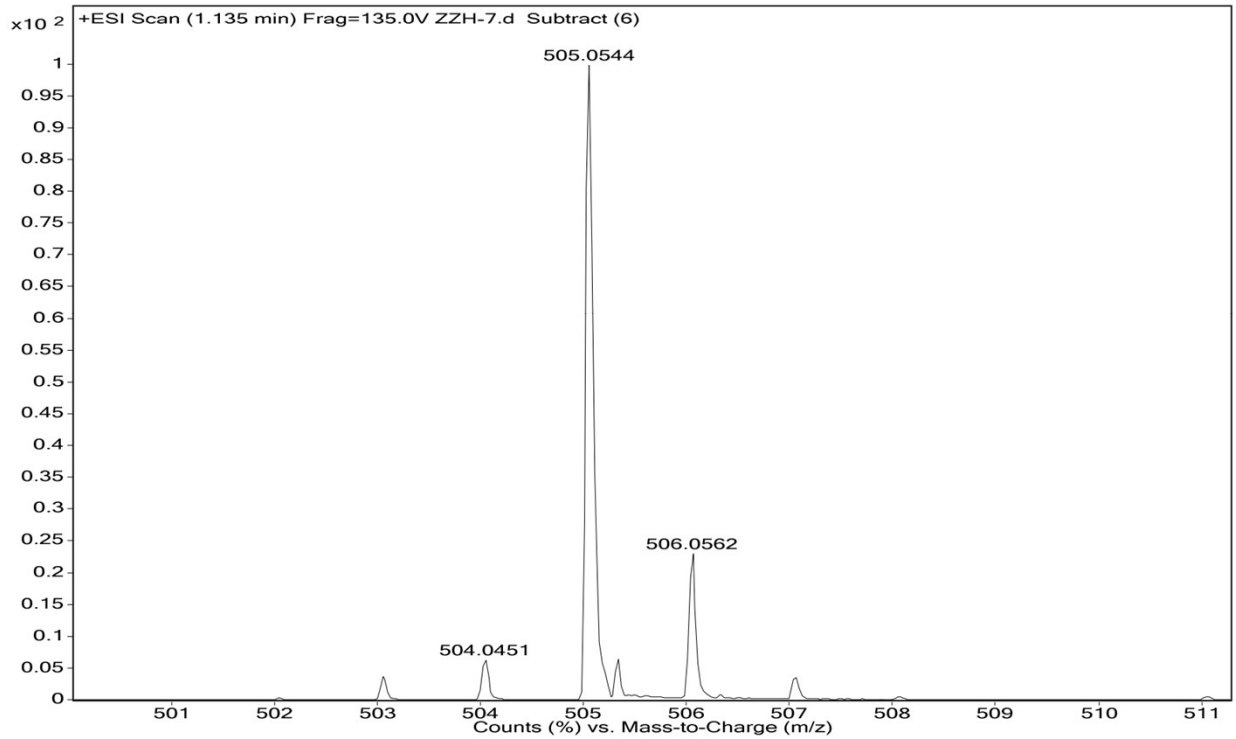

Figure S31. HRMS spectrum of Asp.

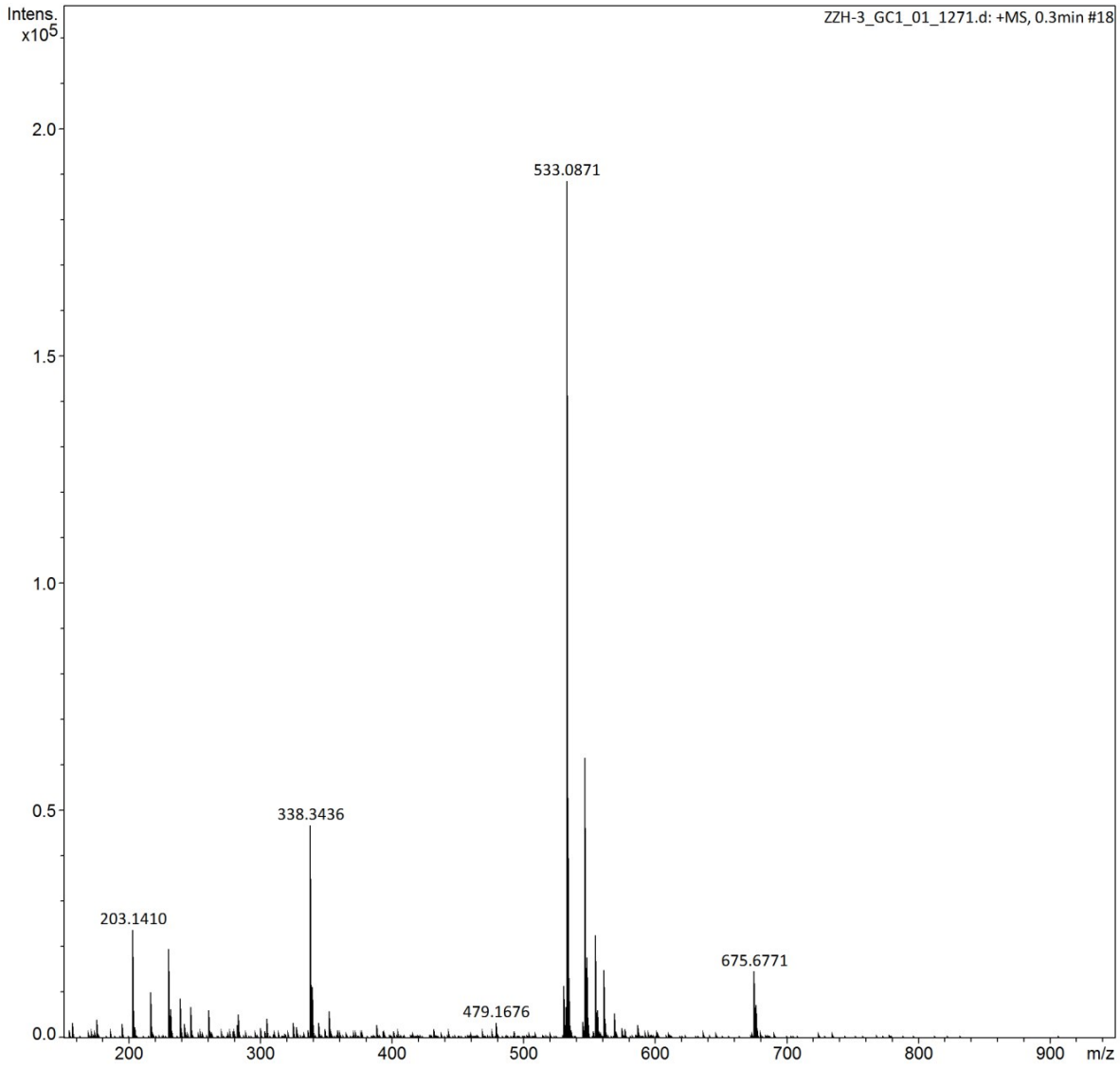

Figure S32. HRMS spectrum of Glu.

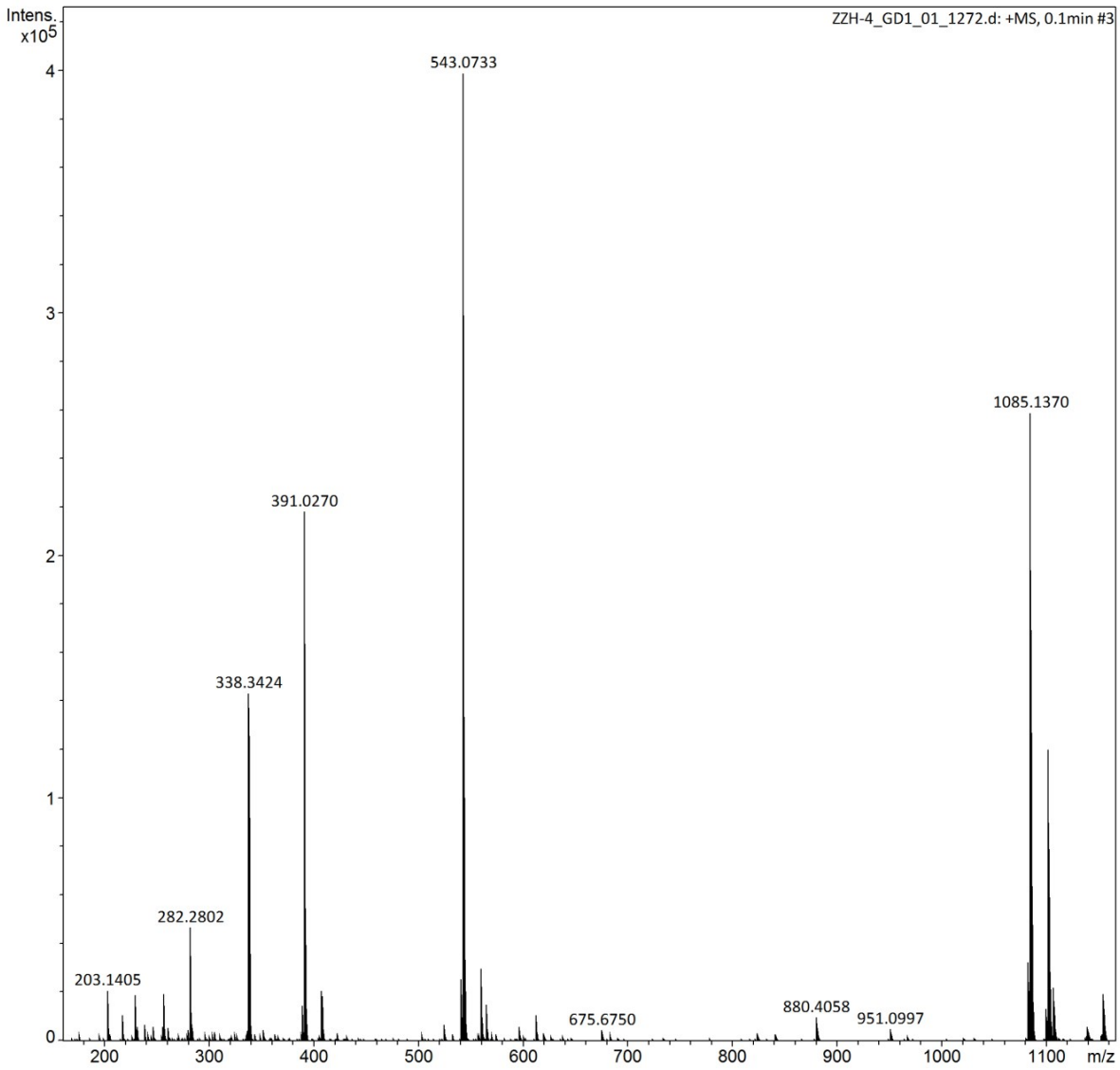

Figure S33. HRMS spectrum of Man.

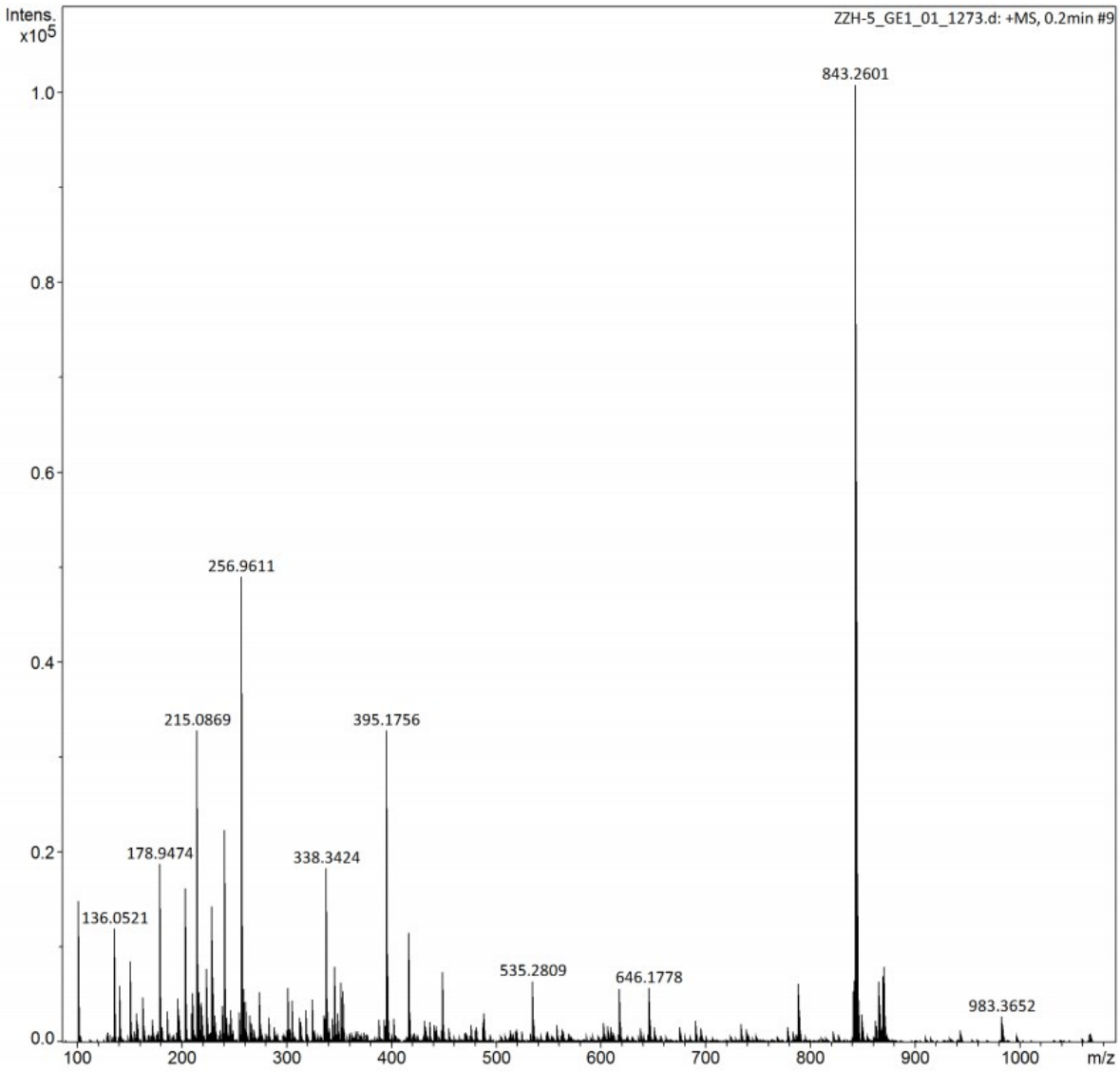

Figure S34. HRMS spectrum of Ala-Py.

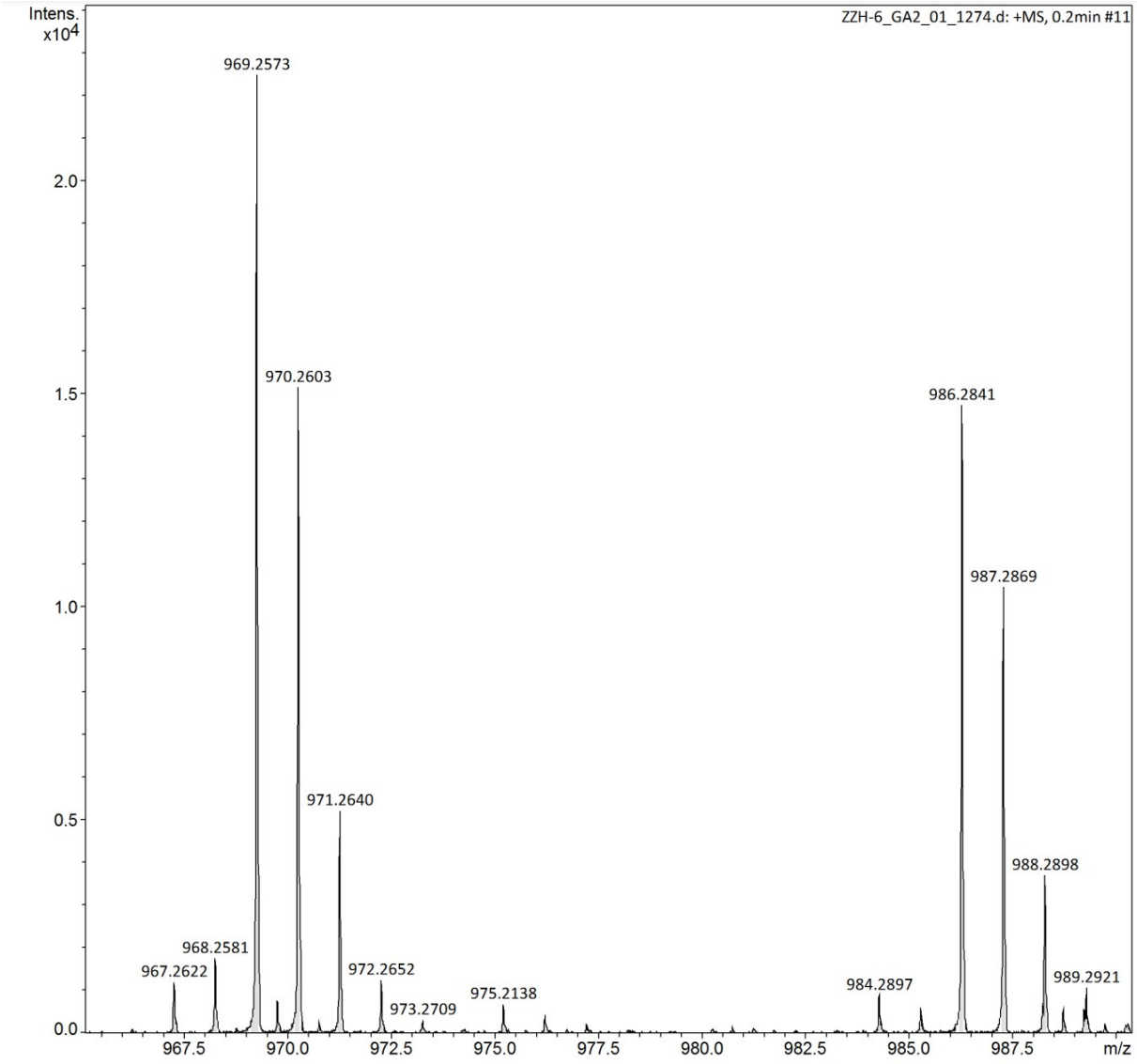

Figure S35. HRMS spectrum of Man-Py.

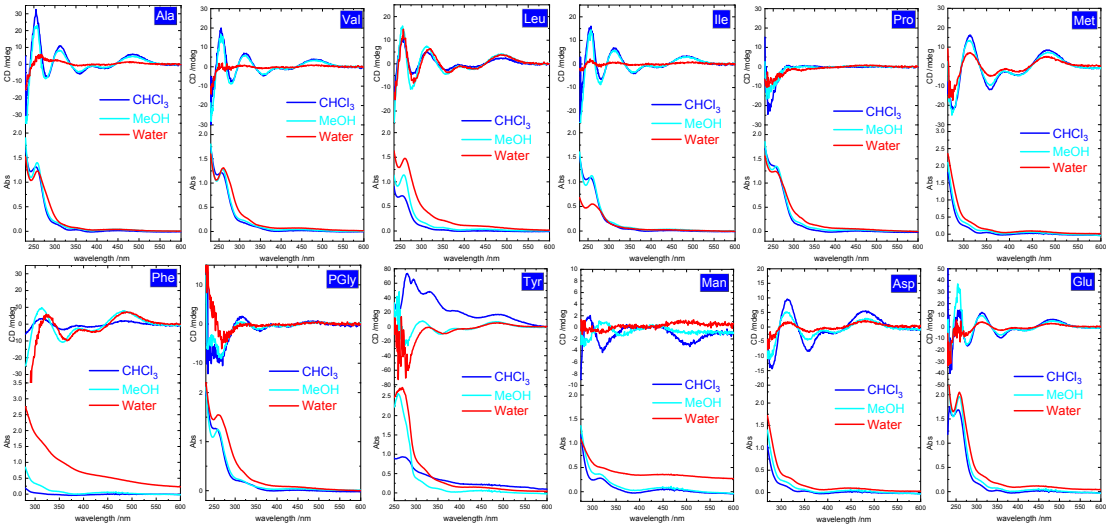

Figure S36. CD spectra of different compounds in different solvents. Concentrations were controlled as 3 mM. It is obvious that Ala, Val, Ile, Met, PGly, Asp and Glu show similar response behaviors towards hydration, of which the mechanism has been illustrated in the main text However, for Leu, Phe and Tyr, the Cotton effects show barely decreasing tendency upon hydration. Apparently, compared to other compounds, phenylalanine, leucine and tyrosine moieties of Phe, Leu and Tyr have relative large hydrophobic domains, which shall hinder the hydration process. Man and Pro, which cannot form Herrick's conformation due to lack of amide groups, possesses weak and abnormal response in water or other solvents, contributed by the flexible substituent arms.

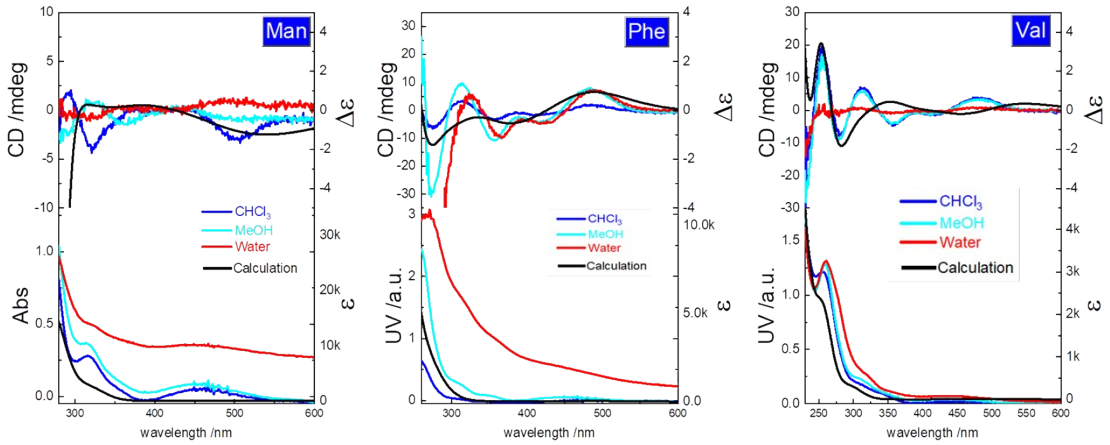

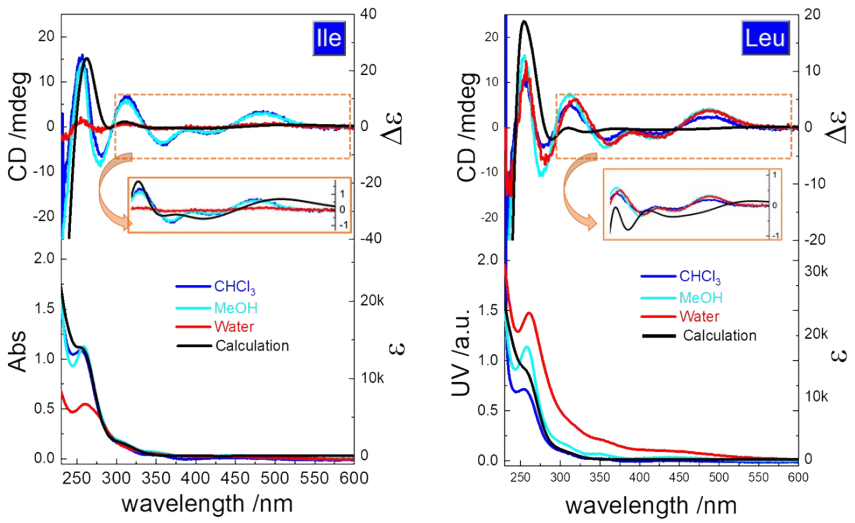

Figure S37. Comparison between experimental and calculated CD spectra of different compounds in different solvents.

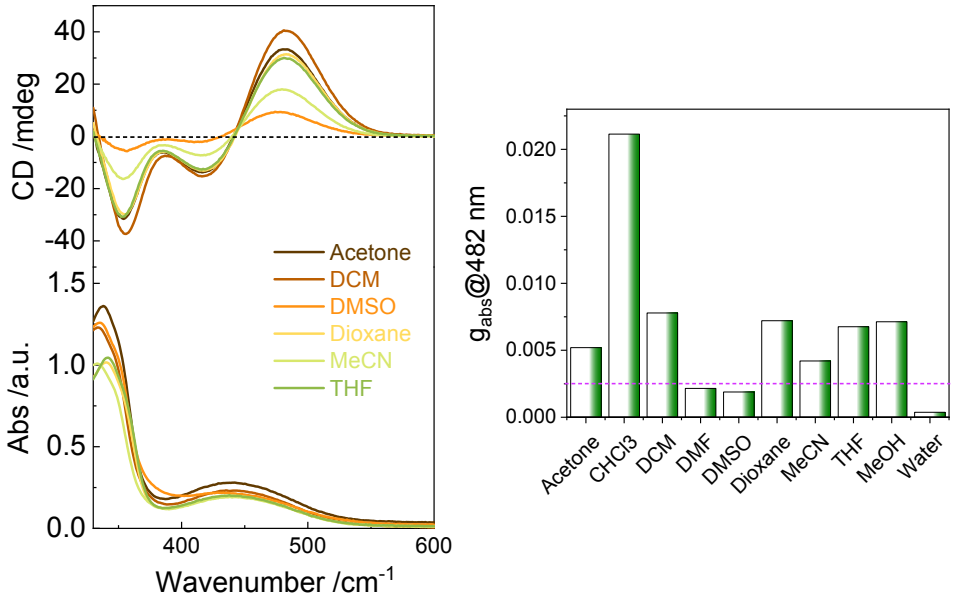

Figure S38. CD spectra and g_{abs} values in different solvents of Ala. [Ala] = 1 mM; l = 10 mm.

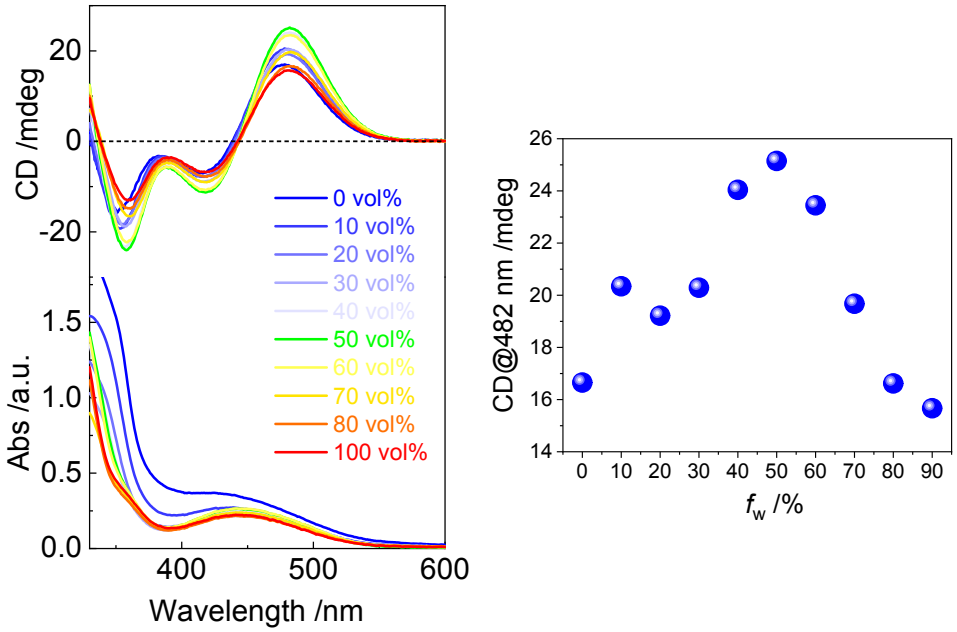

Figure S39. Water fraction-dependent CD spectra against DMF as well as the CD values at 482 nm of Ala. [Ala] = 1 mM; l = 10 mm.

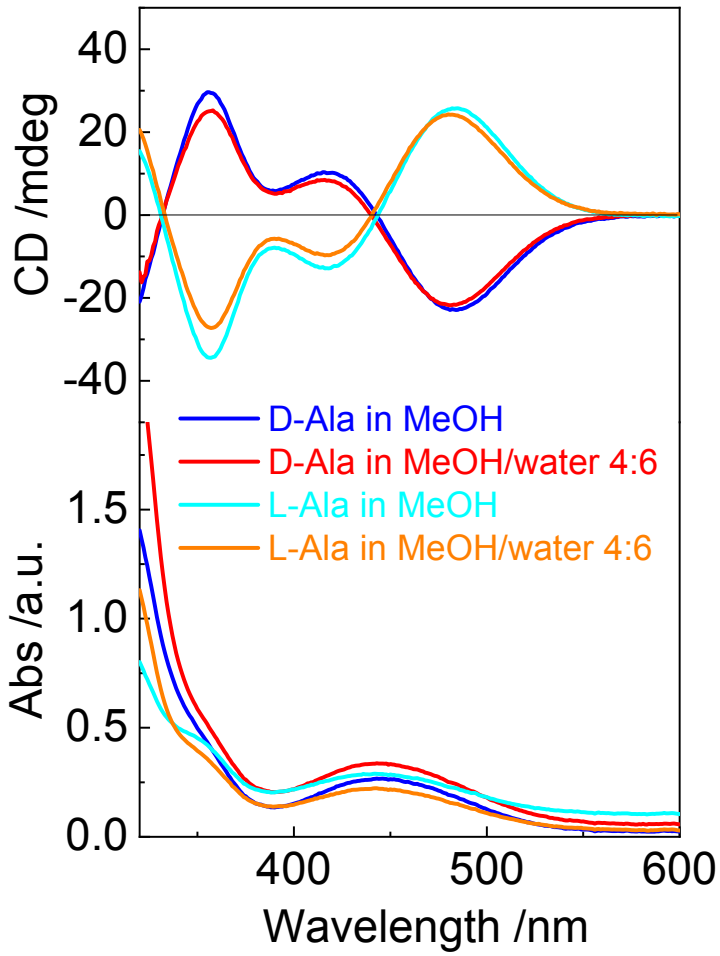

Figure S40. Water fraction-dependent CD spectra of Ala with D- or L-configurations.

[Ala] = 1 mM; *l* = 10 mm.

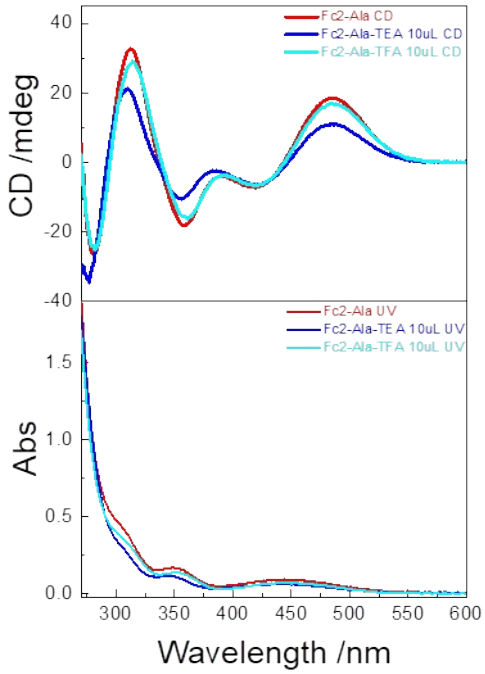

Figure S41. ECD spectra of Ala (3 mM, in $CHCl_3$) with the addition of TEA or TFA individually.

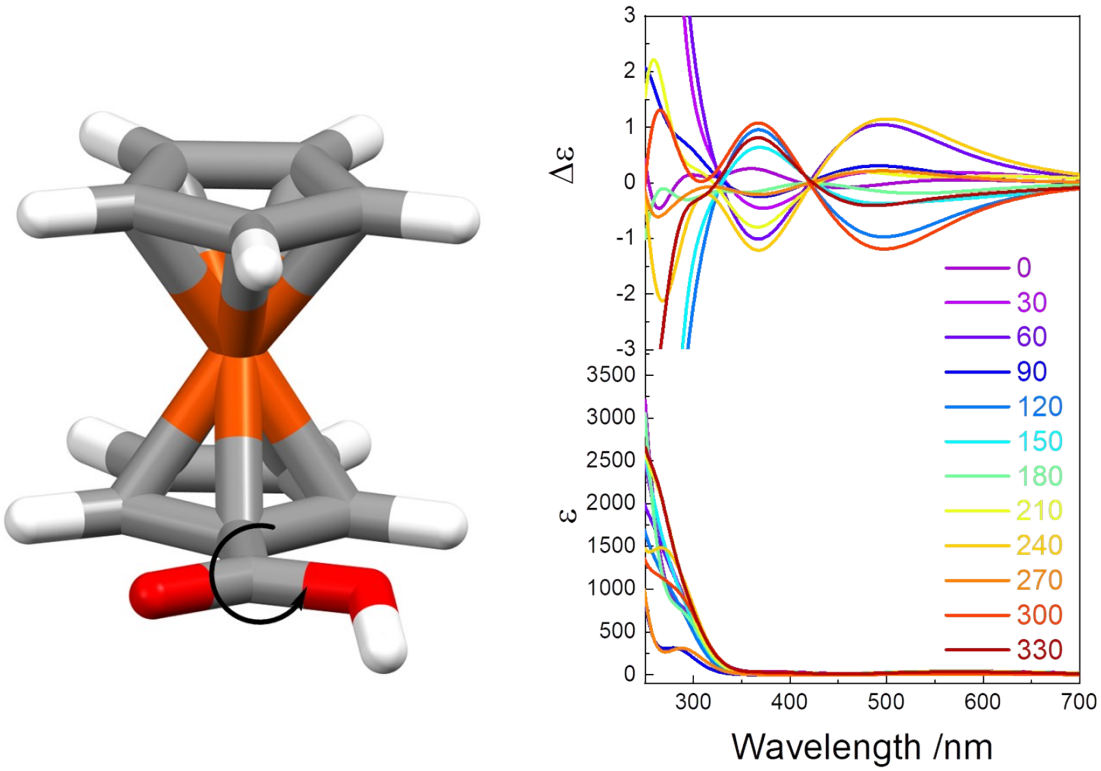

Figure S42. The rotation of ferrocene monocarboxylic acid and the corresponding calculated ECD spectra.

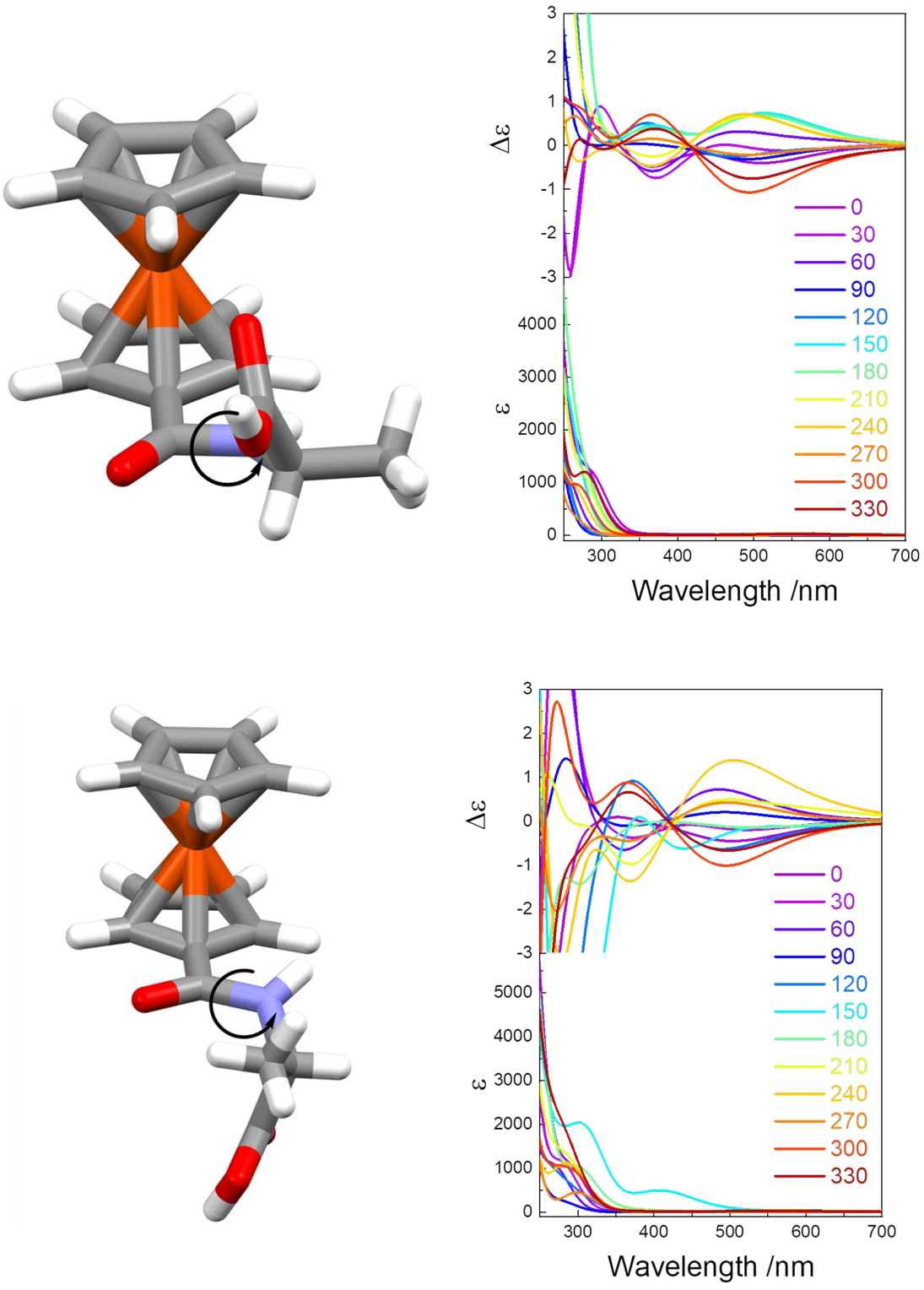

Figure S43. The rotation of ferrocene monoalanine at different positions and the corresponding calculated ECD spectra.

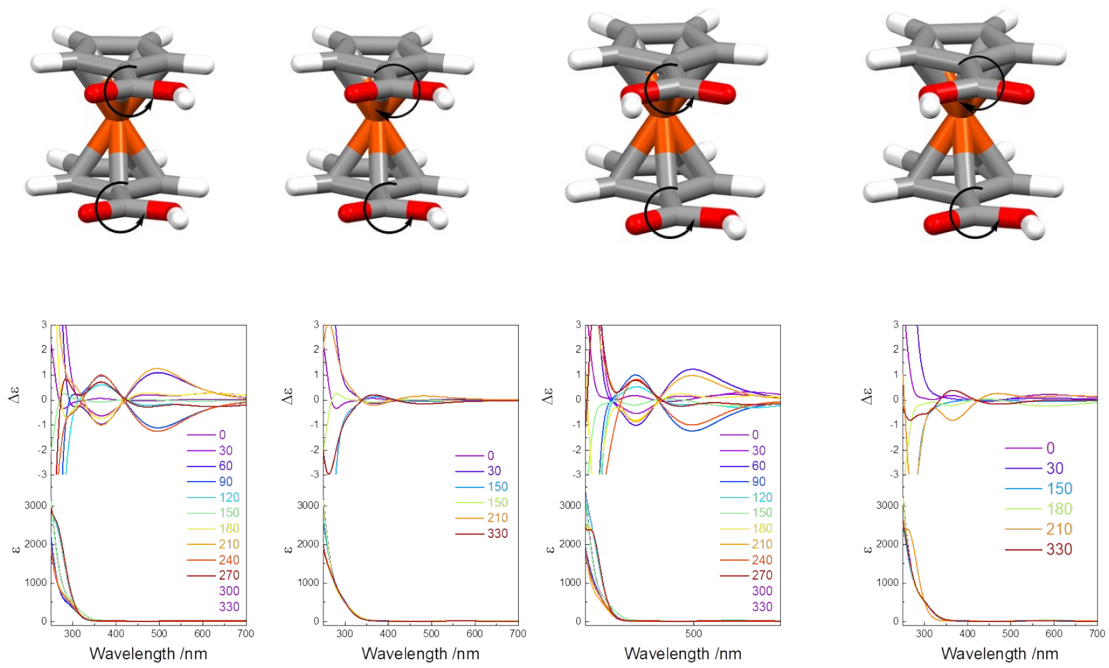

Figure S44. The rotation of ferrocene dicarboxylic acid and the corresponding calculated ECD spectra.

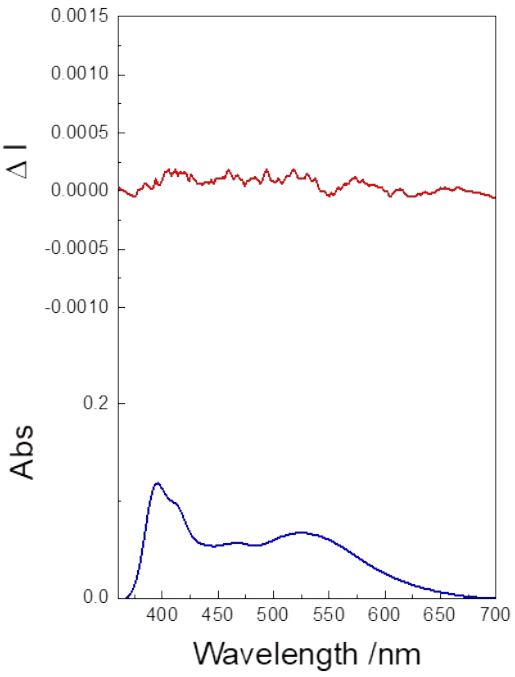

Figure S45. CPL spectra of Man-Py in DMF (3 mM).

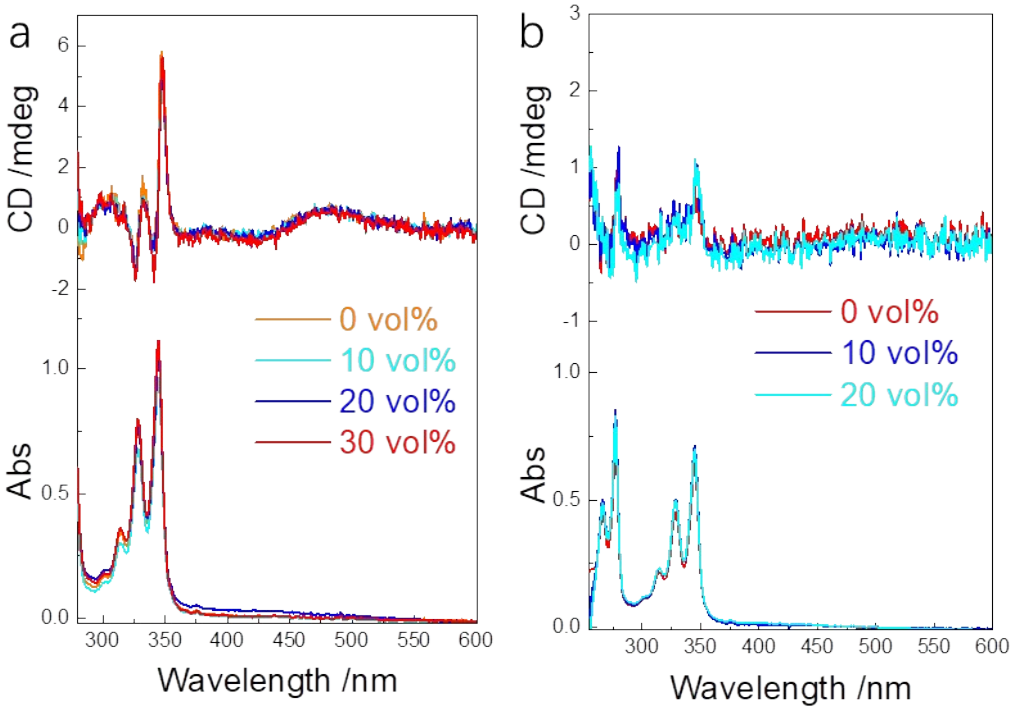

Figure S46. a,b) CD spectra of Ala-Py and Man-Py with different water fractions against DMF.

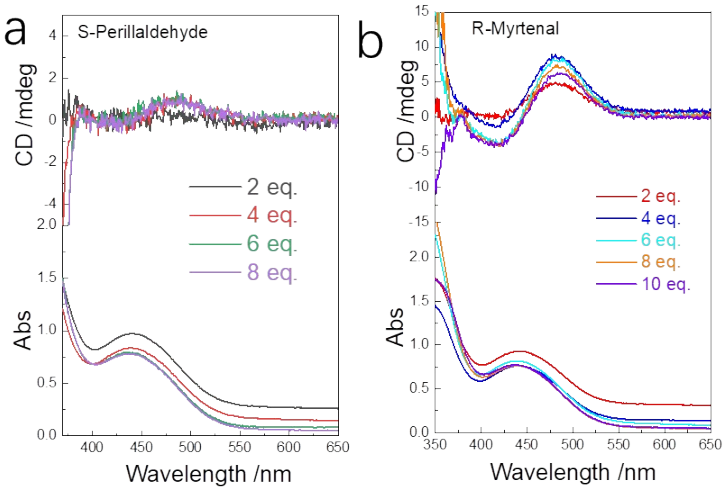

Figure S47. a,b) Molar ratio-dependent CD spectra of different aldehydes in Ala (chloroform, 3 mM).

Table S1 Crystal data of Val.

Deposition Number	2056201

Formula	C22 H28 Fe1 N2 O6
Temperature(K)	173.00(10)
Wavelength	1.54184Å
Crystal system	tetragonal
Space group	P 4_1 2_1 2
a,b,c/Å	**a** 11.8107(6) **b** 11.8107(6) **c** 15.9318(10)
V, Å3	2222.37
Cell angles	α 90.00 β 90.00 γ 90.00
Z, Z'	Z: 4 Z': 0
R-factor (%)	11.99

Table S1 Crystal data of Man.

Deposition Number	2056202
Formula	C28 H22 Fe1 O8
Temperature(K)	173
Wavelength	1.54184Å
Crystal system	orthorhombic
Space group	P 2_1 2_1 2_1
a,b,c/Å	**a** 7.2076(2) **b** 20.5822(5) **c** 21.2269(7)
V, Å3	3148.97
Cell angles	α 90 β 90 γ 90
Z, Z'	Z: 4 Z': 0
R-factor (%)	3.54

Table S1 Crystal data of Ala-Py.

Deposition Number	2056203
Formula	C52 H42 Fe N4 O4,3(C4 H8 O)
Temperature(K)	173
Wavelength	1.54184Å

Crystal system	monoclinic
Space group	I 2
a,b,c/Å	**a** 16.6972(2) **b** 10.48428(16) **c** 30.9632(5)
V, Å3	5336.54
Cell angles	α 90 β 100.0890(14) γ 90
Z, Z'	Z: 4 Z': 0
R-factor (%)	4.38

Table S1 Crystal data of Ile.

Deposition Number	2056204
Formula	C24 H32 Fe1 N2 O6
Temperature(K)	173
Wavelength	1.54184Å
Crystal system	tetragonal
Space group	P 4_1 2_1 2
a,b,c/Å	a 12.1015(2) b 12.1015(2) c 16.0220(5)
V, Å3	2346.36
Cell angles	α 90 β 90 γ 90
Z, Z'	Z: 4 Z': 0
R-factor (%)	4.03

Table S1 Crystal data of Leu.

Deposition Number	2056205
Formula	C24 H32 Fe1 N2 O6,C4 H8 O1
Temperature(K)	173
Wavelength	1.54184Å
Crystal system	orthorhombic
Space group	P 21 21 21
a,b,c/Å	**a** 11.20690(10) **b** 11.43430(10) **c** 22.8029(3)

V, Å3	2922.03
Cell angles	α 90.00 β 90.00 γ 90.00
Z, Z'	Z: 4 Z': 0
R-factor (%)	3.08